RECTIFICATION AND REGISTRATION OF REMOTELY SENSED DATA
(U) AEROSPACE CORP EL SEGUNDO CA ELECTRONICS AND OPTICS
DIV B G KASHEF ET AL. 25 JUN 85 TR-0084A(9975)-1

END

FILMED

DTIC

1·0

2·8

2·5

5·0

3·15

2·2

3·5

1·1

4·0

2·0

4·5

1·8

1·25

1·4
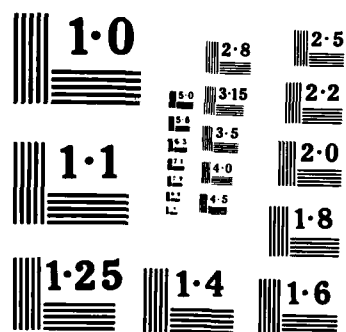
1·6

NATIONAL BUREAU OF STANDARDS
MICROCOPY RESOLUTION TEST CHART

AD-A158 827

Rectification and Registration of Remotely Sensed Data

BAYESTEH G. KASHEF
Electronics and Optics Division
The Aerospace Corporation
El Segundo, CA 90245

and

ALEXANDER A. SAWCHUK
Image Processing Institute
University of Southern California
Los Angeles, CA 90089

25 June 1985

DTIC
ELECTE
SEP 4 1985
B

Final Report

**APPROVED FOR PUBLIC RELEASE;
DISTRIBUTION UNLIMITED**

85 8 29 062

This report was submitted by The Aerospace Corporation, El Segundo, CA
90245, under Contract No. F04701-83-C-0084 with the Space Division, P.O. Box
92960, Worldway Postal Center, Los Angeles, CA 90009. It was reviewed and
approved for The Aerospace Corporation by J. R. Parsons, Principal Director,
Sensor Systems Subdivision, Electronics and Optics Division.

This report has been reviewed by the Public Affairs Office (PAS) and is
releasable to the National Technical Information Service (NTIS). At NTIS, it
will be available to the general public, including foreign nationals.

This technical report has been reviewed and is approved for publication.
Publication of this report does not constitute Air Force approval of the
report's findings or conclusions. It is published only for the exchange and
stimulation of ideas.

FOR THE COMMANDER

GERHARD E. AICHINGER
Technical Advisor
SD/PMR

JAMES A. BORNINO
Chief, Aerospace Contract Management
Office SD/PMR

SECURITY CLASSIFICATION OF THIS PAGE *(When Data Entered)*

REPORT DOCUMENTATION PAGE

READ INSTRUCTIONS BEFORE COMPLETING FORM

1. REPORT NUMBER	2. GOVT ACCESSION NO.	3. RECIPIENT'S CATALOG NUMBER
SD-TR-85-40	AD·A158 827	

4. TITLE *(and Subtitle)*	5. TYPE OF REPORT & PERIOD COVERED
RECTIFICATION AND REGISTRATION OF REMOTELY SENSED DATA	Final
	6. PERFORMING ORG. REPORT NUMBER
	TR-0084A(9975)-1

7. AUTHOR(*s*)	8. CONTRACT OR GRANT NUMBER(*s*)
Beysteh G. Kashef and Alexander A. Sawchuk	F04701-83-C-0084

9. PERFORMING ORGANIZATION NAME AND ADDRESS	10. PROGRAM ELEMENT, PROJECT, TASK AREA & WORK UNIT NUMBERS
The Aerospace Corporation El Segundo, Calif. 90245	

11. CONTROLLING OFFICE NAME AND ADDRESS	12. REPORT DATE
Space Division Los Angeles Air Force Station Los Angeles, Calif. 90009-2960	25 June 1985
	13. NUMBER OF PAGES 87

14. MONITORING AGENCY NAME & ADDRESS*(if different from Controlling Office)*	15. SECURITY CLASS. *(of this report)*
	Unclassified
	15a. DECLASSIFICATION/DOWNGRADING SCHEDULE

16. DISTRIBUTION STATEMENT *(of this Report)*

Approved for public release; distribution unlimited

17. DISTRIBUTION STATEMENT *(of the abstract entered in Block 20, if different from Report)*

18. SUPPLEMENTARY NOTES

19. KEY WORDS *(Continue on reverse side if necessary and identify by block number)*

Image rectification	Artificial intelligence
Image registration	Resampling
Mapping	Change detection
Geometrical distortions	Multisensor
Signal processing	Synthetic aperture radar imagery

20. ABSTRACT *(Continue on reverse side if necessary and identify by block number)*

An important problem in any onboard imaging system is the rectification and registration of images generated by onboard sensors. Accurate registration is a key requirement for detecting changes (in position, brightness, texture, boundary, etc.), from one sensed image to the next, as well as classification of data for intelligence gathering and vehicle guidance.

This report discusses techniques of finding match points in pairs of images and performing geometric corrections and unwarping to compensate for systematic

DD FORM **1473**
(FACSIMILE)

SECURITY CLASSIFICATION OF THIS PAGE *(When Data Entered)*

19. KEY WORDS (Continued)

20. ABSTRACT (Continued)

and random variations in the flight path, ephemeris, and sensor response. Techniques of resampling and interpolation of image data are reviewed, and the particular characteristics of sensors operating over a wide spectrum from visible through infrared and microwave are discussed. Particular attention is given to the rectification and registration of synthetic aperture radar (SAR) imagery, and several future study tasks on this specialized area are outlined.

CONTENTS

CONTENTS (Continued)

FIGURES

3

FIGURES (Continued)

TABLES

DTIC
SELECTED
SEP 4   1985

B

I. INTRODUCTION

Two images of the same region are said to be _registered_ when equivalent geographic points of the scenes in the two images coincide.

Rectification is a congruencing process by which the geometry of the image is made planimetric, i.e., where the two images of the same scene are transformed so that the size and shape of any object on one image is the same as the size and shape of that object on the other image. Image rectification allows a direct comparison of different images of the same scene either originating from different sensors or from the same sensor but under different conditions (e.g., orientation, season, weather, time of day).

Raw, unprocessed images cannot be registered directly because of differences in viewing conditions, and because of radiometric and geometrical distortions (warping). A preprocessing or "unwarping" of the image data before registration and information extraction, in the form of geometric and radiometric corrections and data processing (interpolation, resampling, reformatting), is necessary. This process of rectification, in addition to registration and change detection, is the subject of this report.

The accurate rectification/registration of data is a key requirement for several applications such as intelligence gathering, advanced vehicle guidance, change detection, and classification of remotely sensed data.

A. STUDY OBJECTIVES

The objective of the study is to evaluate the feasibility of a rectification system having pixel (picture element) to subpixel registration accuracy and semiautomatic operation in a multisensor environment. Special consideration was given to ground-based, mobile, compact systems with near real-time processing.

The purpose of the first phase of this study was to investigate the general process of rectification/registration of remotely sensed, high resolution data in a multisensor environment and in the presence of multitemporal geometric distortions. Specific sensors under consideration in this phase of

7

the study are very general and generic in nature, covering the whole spectrum from optical/near infrared (IR) to middle IR, thermal IR, and microwave, including both active types (sensor providing its own source of electro-magnetic radiation) and passive types (sensor using naturally reflected energy from the terrain).

In the second phase of the study, the emphasis was placed on the use of synthetic aperture radar (SAR) for imaging as a sole sensor. The purpose was to study the specific qualities and problems of SAR matching and registration techniques in order to analyze the state of the art of rectification algorithms and to propose some future tasks in this area.

B. STUDY APPROACH

To achieve the objectives, a step-by-step approach was taken, and the following tasks have been accomplished:

- Literature survey of rectification and registration techniques in use today and identification of the state of the art.

- Identification and study of candidate techniques or a combination of several algorithms from the wealth of techniques available. This spectrum ranges from classical correction methods to feature matching to hybrid techniques.

- Evaluation of error removal capabilities of image-matching algorithms under various geometric distortions and dependency of sensors to different errors.

- Study of the effect of various resampling/interpolation algorithms on registration accuracy.

- Detailed study of map-matching methods specific to SAR imagery.

- Preliminary study of change detection techniques.

- Preliminary study and analysis in the areas of signal processing and artificial intelligence to identify novel techniques for the removal of speckle and handling of variations in contrast. The existence of these factors lead to grossly incorrect matches. (Speckle is a granular noise arising from the random interference of wavefronts scattered from an optically rough surface.)

- Identification of several future approaches and techniques which include SAR image matching to other SAR images, to visible references, or to forward looking infrared (FLIR) reference images.

8

C.   OVERVIEW

A typical data gathering system geometry for remote sensing applications
is depicted in Figure 1. A reference map is provided by platform A with an
onboard sensor. Prior to the remote sensing operation, this reference map
covers a much larger area than the target or the scene of interest, and is
constructed and preprocessed accurately and is stored in the computer on the
ground. A sensed image is generated by a second sensor on board platform B.
This sensed image contains the target or the scene of interest only and is
contained somewhere within the boundaries of the reference map. The problem
is to rectify and correct the sensed image in such a way that accurate regis-
tration of all points within the sensed image (with respect to the reference
map) is possible. Rectification/registration can be accomplished on a com-
puter located in a mobile station on the ground.

This report covers the area of image rectification, registration, and
change detection for images generated by onboard sensors. Types of sensors
under consideration in the first phase of the study were very general and
generic in nature, covering the whole spectrum from optical to IR to microwave
(sections I through V). In the second phase of the study, specific problems
of SAR registration and rectification were surveyed and studied (section VI),
and new future tasks were proposed (section VII).

The conclusion of the study is covered in the first section of the
report, along with the introduction, objectives, and overview.

Section II describes the process of rectification as a whole. The
sources of image distortion are examined and various bases of reference data
are considered.

Section III describes geometrical distortion in imaging systems due to
optical and orientation effects. A design concept for near-real-time correc-
tion is also presented. Correction for display and matching is considered,
system hardware requirements are described, and superposition of multiple
images is discussed.

9
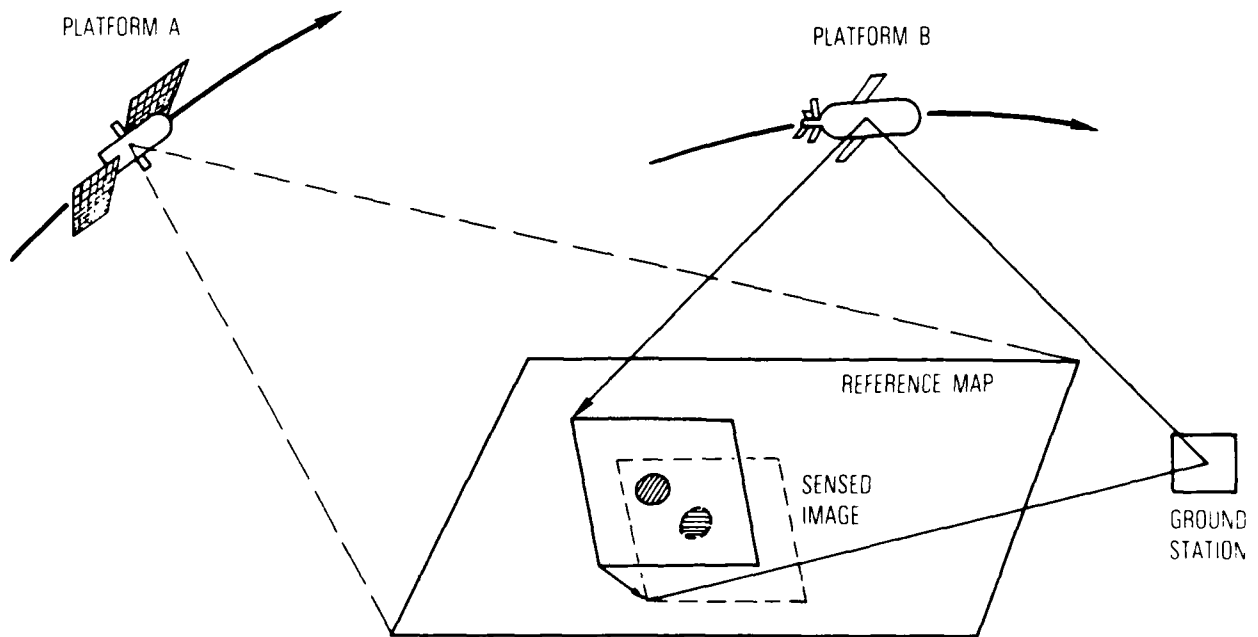
Figure 1. Typical Data Acquisition System

In general, three basic types of rectification algorithms have emerged from this study and are categorized into: signal processing-based, artificial intelligence-based, and hybrid techniques which make the best use of the first two approaches. Section IV describes all three categories of image matching as well as change detection algorithms for multisensor environments.

In real-time systems using high data rates, rectification of every picture element is not practical. In these systems, only a fraction of samples are fully corrected geometrically, and remaining samples are obtained using interpolation, resampling, or statistical approximation means. In section V an overview of the resampling process as it relates to registration and rectification of onboard sensor imagery is discussed. Various one- and two-dimensional resampling techniques are reviewed and compared.

Very little work is available on the matching of SAR images to visible images or to a SAR reference map. Most of the previous work has been concentrated in the rectification and registration of visible imagery as discussed in sections II through V. Section VI of this report deals with specific qualities of SAR imagery which may cause serious problems in accurate image matching and investigates the feasibilities of various rectification, registration, and change detection algorithms applicable to SAR imagery.

Part of the objective of the second phase of this study is to propose and develop techniques for registration and change detection with SAR images. These techniques may include SAR image matching to other SAR reference images, to visible references, or to FLIR reference images. Because the problem is generally quite difficult and little work has been previously done on the problem, several possible approaches are proposed in section VII.

Based on analysis in the areas of signal processing and artificial intelligence, four specific tasks are proposed for image registration/rectification and possible change detection of SAR data:

- The first task involves registration through geometrical transformation and resampling.

- The second task, which requires considerable research effort, involves total registration and change detection through a combination of signal processing and artificial intelligence techniques.

11

- The third task is basically a simplified version of the second task for registration of SAR images with a known, well-defined visible image.

- The last task involves man-machine interactive methods for image rectification. This approach to rectification allows for analytical evaluation and comparison of various registration algorithms and their performance in addition to the utilization of a photointerpreter's inputs to the system.

D. CONCLUSIONS AND RESULTS

This study has surveyed the entire field of image matching, rectification, and registration, including techniques that are applicable to a wide range of sensor wavelengths, image noise levels, image detail, and image distortion. An important conclusion is that there is no universally robust technique or even a family of techniques that can solve all rectification/registration problems. The optimum solution is highly dependent on the particular parameters of the system, including: speed; the number of pixels (resolution); the quality of the reference and sensed images; the size of the processor, including computing, memory and input/output capabilities; the amount of human interaction allowed; and the amount of a priori information available.

The study has led to the emergence of three major types of registration algorithms:

- Correlated or signal-processing-based techniques that numerically compute a measure of similarity between images on a pixel-by-pixel basis

- Artificial intelligence (AI) or feature-based techniques. These methods compute similarity between features extracted from the images. The features can include edges, boundaries, and vertices, and matching is often done at a higher (symbolic) level

- Hybrid techniques, which combine the first two techniques in a hierarchy of levels to make the best use of both.

In general, the feature matching methods work best on images with high signal-to-noise ratio (SNR) regardless of wavelength. Most SAR images never have SNR adequate for a direct application of feature matching techniques. The

12

correlation-based techniques work best on images with low SNR, where they provide some inherent noise suppression. They will also fail, however, if there are significant differences in orientation, magnification, illumination, etc., between reference and search images. Hybrid techniques are needed for low-to-moderate SNR situations, regardless of the utilized wavelength.

Very little has been done on the specific problem of SAR rectification and registration. It is generally a very difficult problem that requires a great deal more research and development. The many unanswered questions about SAR need more analysis, simulation, and experimental verification. There is research at many levels (up to the doctoral dissertation level) under way at many organizations to find out some of these answers, but they do not come easily. Some of the specific questions and tasks discussed in this study could easily consume several man-years of effort. Many of the most useful practical results have involved extensive software development taking place over a period of years.

On a more positive side, however, with specific well-defined information about a particular scenario for matching, rectification, and registration, it may be possible to find a reasonable practical solution that, although not optimal, will give a reasonably good result.

13

II. RECTIFICATION/REGISTRATION OVERVIEW

An important image processing technique is the rectification of imagery generated by various sensors. Rectification methods are usually categorized under the more general term of "preprocessing" techniques. All preprocessing techniques involve modifying an image to make it more like an "ideal" image, which is the first step of visual data processing. Its objectives are: (a) reconstruction of the ideal, high fidelity image from the low-quality, distorted input image; and (b) improvement or enhancement of the quality of the input image by suppressing noise and emphasizing selected features to facilitate later stages of image processing. Preprocessing involves three kinds of modification: rectification, gray-level modification, and sharpening/smoothing operations. Gray-level (or intensity) correction compensates for the nonuniformity of sensor sensitivity and contrast. Sharpening and smoothing are important for edge detection and other types of feature extraction.

In this section, the process of rectification as a whole is reviewed, the sources of image distortion are examined, and formation of useful data bases for specific map-matching problems is considered.

A. CATEGORIES OF ERRORS

Numerous error sources contribute in the existing distortions in an unprocessed sensed image when compared to a preprocessed reference map of the same region. These error sources are grouped into four convenient categories according to Conrow and Ratkovic [1] as depicted in Table 1. These categories are global, regional, local, and nonstructured errors.

Global errors affect intensity levels of all elements of the scene uniformly and can generally be removed by the rectification process. These errors include geometrical and radiometrical (gain/bias) distortions.

The second category, called regional errors, uniformly affects the intensity levels within homogeneous regions only and not the whole scene as with global errors. An example of this category is "contrast reversals" which

15

Table 1. Categories of Errors in Image Matching

	GLOBAL ERRORS	REGIONAL ERRORS	LOCAL ERRORS	NONSTRUCTURED
DEFINITION	AFFECTS INTENSITY LEVEL OF ALL SCENE ELEMENTS UNIFORMLY	AFFECTS INTENSITY LEVEL UNIFORMLY WITHIN HOMOGENEOUS REGIONS	AFFECTS EACH PIXEL INDEPENDENTLY WITHIN A SMALL REGION	ALL OTHER ERROR SOURCES
EXAMPLE	• GEOMETRICAL DISTORTIONS • RADIOMETRIC DISTORTION	• CONTRAST REVERSALS	• ADDITIVE NOISE • SPECKLE	• CLOUD OVER PORTIONS OF TARGET AREA
ERROR REMOVAL	← RECTIFICATION PROCESS →			

affect the sensed image such that the relative order of intensities between the two images to be compared is not preserved. This can occur in infrared images acquired at different times of the day or in cases where a SAR image is compared with a visible image of the same scene. A significant variation in contrast may lead to grossly incorrect matches. There are some possibilities of error removal in this case through edge-matching algorithms and cluster-reward techniques that are described later.

Local errors are the third category of errors. Local errors affect each pixel within a small region independently. Additive noise and speckle in SAR imagery come under this category. The spatial size of the speckle is generally on the order of the limiting resolution of the coherent SAR imaging system, and this signal-dependent coherent-noise makes rectification and restoration of SAR images more difficult. Some algorithms are available for the partial removal of speckle available, and these are discussed in section VII.

The last grouping of errors, called nonstructured errors, covers all other error sources not already included in the global, regional, or local categories. An example is a cloud over portions of the region of interest. However, some rectification algorithms (correlation type or hybrid type) can still perform even under the condition that part of the scene in the sensed image is missing (under the cloud).

B. TYPES OF DISTORTIONS REMOVED BY RECTIFICATION

A sequence of images of the same scene taken at different times by the same sensor will contain relative distortions because of differences in the viewing and scanning conditions at the sensor. These distortions are in addition to other variations and error sources as discussed in the previous section. Generally, radiometric and geometric distortions (which are in the category of global errors) can be accommodated by rectification and pre-processing, whereas all other types of errors can be removed somewhat through the right choice of algorithm [1]. This section discusses details of radiometric and geometric distortions.

17

1. RADIOMETRIC DISTORTIONS

These distortions are caused by atmospheric- and sensor-induced
filtering, sensor imperfections, camera or scanner shading effects (nonuniform
responses), detector gain variations, and sensor detection gain errors.
Radiometric distortions appear in the form of blemishes, horizontal stripes,
shading, and nonuniform intensity distributions. Radiometric intensity
corrections for nonuniform sensor sensitivity can be implemented in real-time
using simple table lookup techniques [1-3]. Bias and gain error compensations
can also be implemented in the same manner. The effects of some of these dis-
tortions on the image are shown in Figure 2.

Radiometric distortions are generally predictable and can be corrected
relatively easily. Radiometric corrections are described in detail primarily
in the remote sensing literature [1,2]. The following sections of the report
deal mainly with geometric corrections of data, including the analysis of new
techniques available and their error removal capabilities. The radiometric
errors are considered predictable and correctable.

2. GEOMETRIC DISTORTIONS

The primary causes of geometric distortion are:

●   Sensor related distortion

●   Alignment variation

●   Attitude variation of the spacecraft

●   Ephemeris variation

Image distortion will result in a corresponding registration error if the
distortion is not estimated and removed. The effects of some of these distor-
tions are shown in Figure 2.

a. Sensor Related. Variation in the motion of the sensor over succes
    sive passes introduces distortions. For example, stretching or
    compression of pixel spacing within a scan line results from varia-
    tions in the velocity of the scanner. Another example of distortion
    is the spacing between scan lines which can change from one image to

18
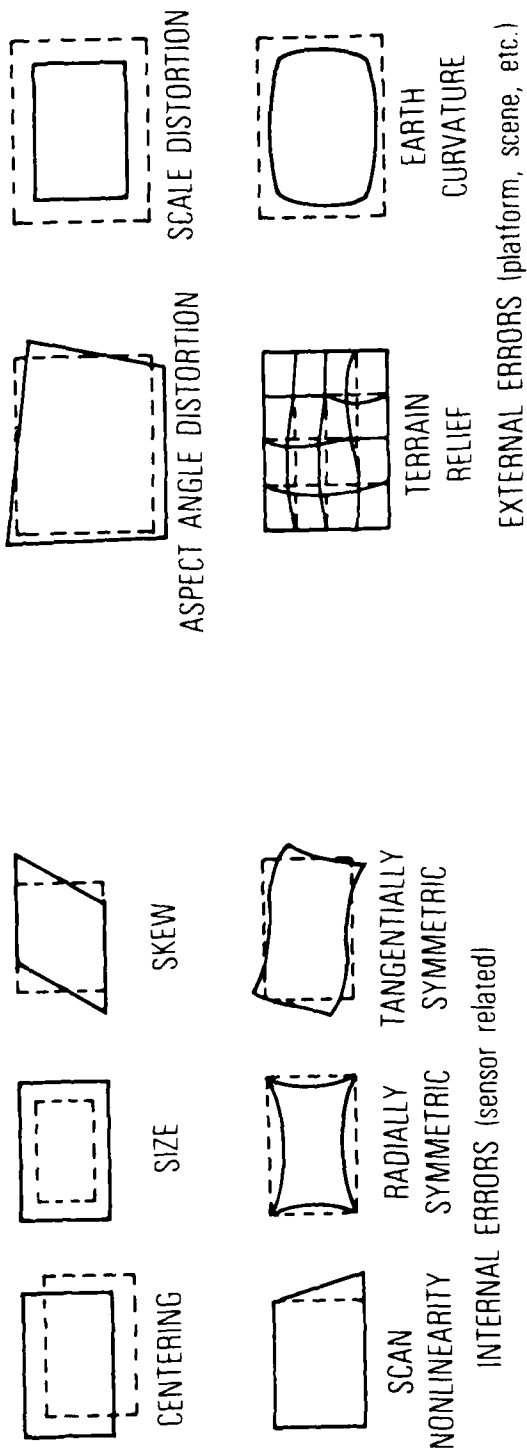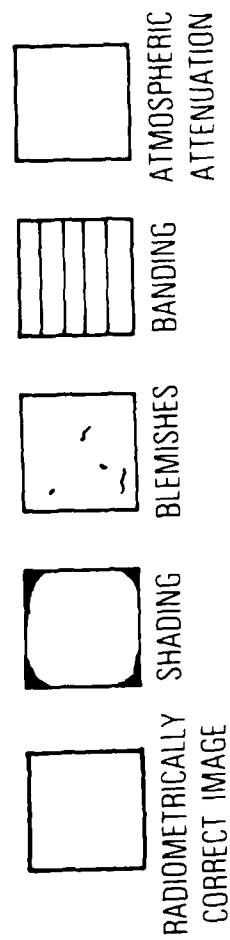
Figure 2. Characteristics of Image Distortions

the other as a result of variations in scan period. The angular velocity of the scan also produces distortions in the form of irregularly spaced pixels in the output image.

b. **Alignment Variation.** The variation in alignment of the sensor with respect to the spacecraft coordinates axes results in both long term drift and short term variations.

c. **Attitude Variation.** Variation in the spacecraft attitude (yaw, roll, and pitch) with respect to a previous pass will cause registration error.

d. **Ephemeris Variation.** This results from variations in the location of the platform with respect to the ground with successive passes over a given region. This error must be corrected for the rectification and comparison of different images.

C. RECTIFICATION/REGISTRATION PROCESS

The general process of rectification for a multisensor environment is shown in Figure 3.

The first step of the process is to match a sensed image to a reference image. The reference image is typically larger than the sensed image, and the sensed image may have magnification or rotation differences or may be geometrically distorted compared to the reference. If a priori geometrical distortion information is available (from calibration or inflight data, for example), it can be used to greatly simplify the matching process. In effect, any a priori knowledge reduces the number of degrees of freedom in the search.

Following corrections from a priori information, or directly starting with the original sensed image, the matching process begins by comparing portions of the sensed image to the reference. Typically, recognizable features in the sensed image such as lines, vertices, edges, or shapes are compared to the reference to find a set of "match point" pairs that can be identified in both images. By matching only portions of the sensed image to the reference, computations are reduced considerably, and the matching is made resistant to minor differences in magnification, rotation, and distortion.

Image matching algorithms (correlation, symbolic matching, or hybrid) are used to compute the location of an _observed_ match-point (i.e., control point or tie point) on the sensed image from the _actual_ match points. The actual

20
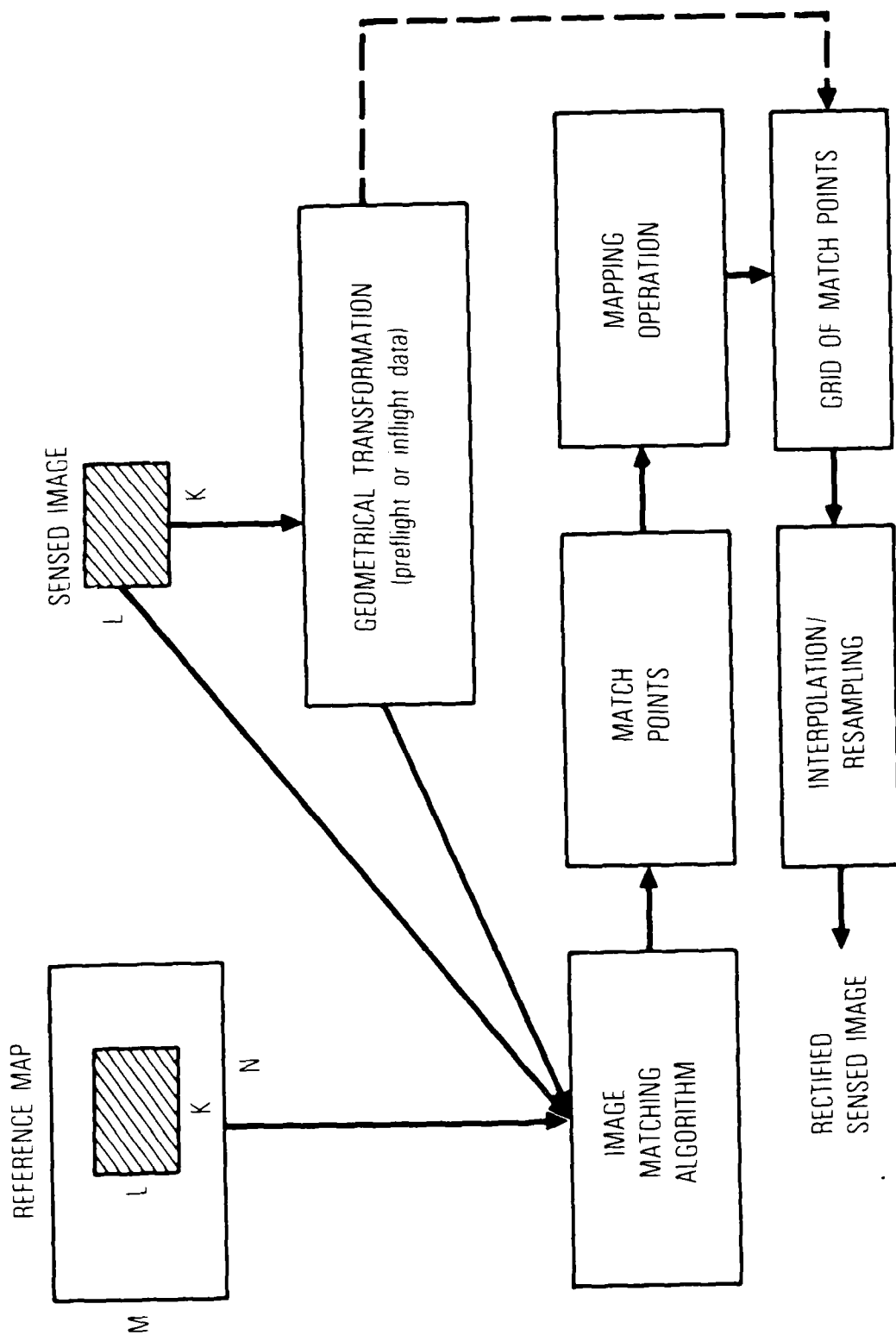
Figure 3. Rectification Process

match points are physical features detectable in the reference map, whose elevations and locations are known precisely.

As shown in Figure 3, after the "match-point" pairs are found, a mapping operation is performed. In this step, several match points, which are distributed on an irregularly spaced mesh of points, are used to calculate a mapping function, relating points on the sensed image to corresponding points on the reference map. This is achieved through a set of distortion functions that are generally piecewise or global polynomials, generally having terms up to and including cubic powers of coordinate variables. More details on the distortion functions are given in section III.

After match point pairs and distortion functions are found, the next step is to perform a resampling operation on the sensed image pixels to register it with the reference image. An interpolation in spatial coordinates is performed on the irregular grid of sensed image match points to determine the location of pixels that are geometrically transformed to a rectified coordinate system. These pixel locations will generally never fall exactly on a pixel location in the sensed image, so interpolation or resampling is performed to obtain an output intensity value for the corrected pixel. Several methods of interpolation with different amounts of smoothing are available.

Section V of this report is an overview of the resampling process as it relates to registration and rectification of sensed imagery. Various one- and two-dimensional interpolation/resampling techniques are reviewed and compared in detail.

D. DATA BASE FORMATION

Wide variations in temporal and spatial characteristics of a scene or region of the terrain make it very difficult to develop a complete data base toward a fully automated rectification system. Nevertheless, some useful data bases for specific map-matching problems are available [1-7].

Figure 4 shows a possible reference data base (i.e., a reference map) which includes operator annotations, vector/graphics, and gray-level image data. Figure 5 shows a more general data base including types of target, temporal signature variation, sensor wavelengths, and material interfaces.

22

OPERATOR ANNOTATIONS

- VECTOR DATA
- RASTER DATA

REFERENCE MAP

VECTOR/RASTER GRAPHICS

- NATURAL FEATURES
- MAPS
- BOUNDARIES
- CONTOURS
- SYMBOLS

GRAY-LEVEL IMAGE DATA

- SATELLITE DATA
- AIRCRAFT DATA

Figure 4. Reference Data Base

TARGET TYPE

STATISTICALLY
REPRESENTATIVE SET
OF REFERENCE MAPS

SENSOR WAVELENGTH

ONE DATA BASE PER
SENSOR WAVELENGTH

DATA
BASE

TEMPORAL SIGNATURE VARIATION

SET OF SENSOR
IMAGES COVERING THE
TOTAL RANGE OF
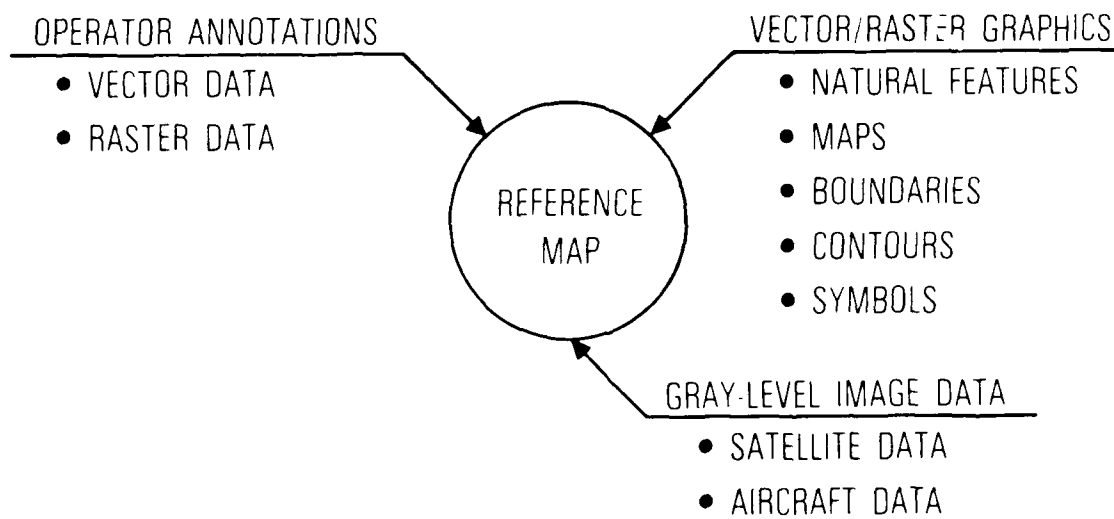VARIATION

MATERIALS/INTERFACES

STATISTICALLY
REPRESENTATIVE SET
OF REFERENCE MAPS
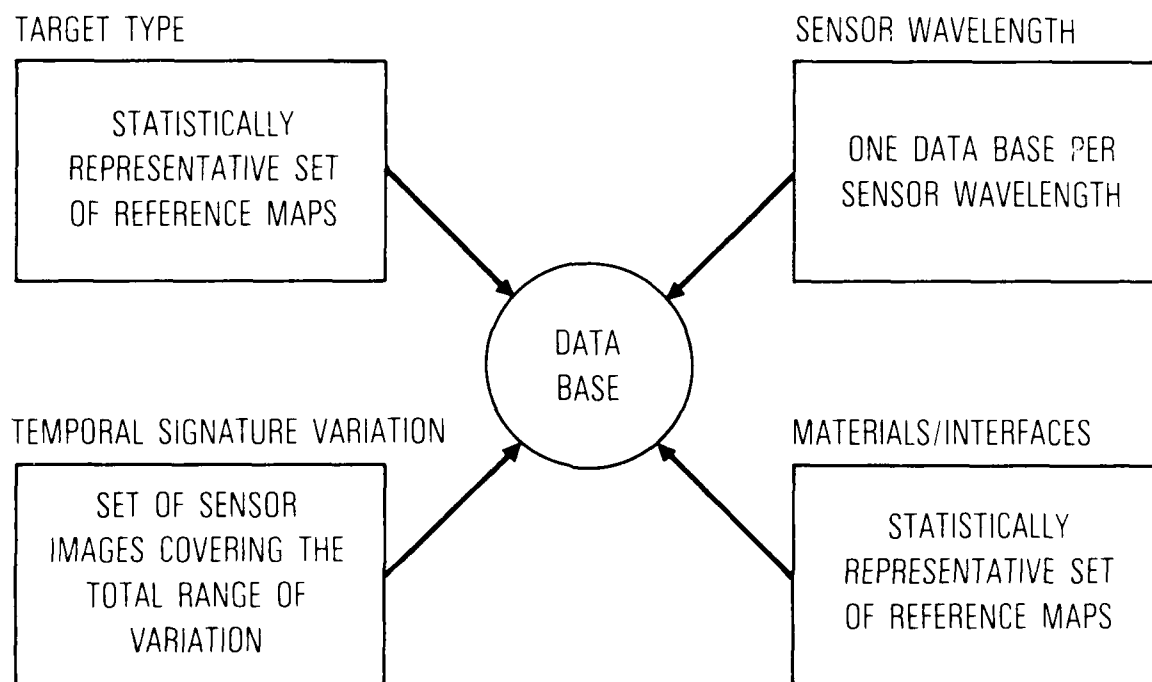
Figure 5. Data Base Formation

III. REAL-TIME GEOMETRIC CORRECTION

In this section, geometrical distortion in imaging systems due to optical and orientation effects is described, and design concepts for near-real-time correction are presented. Correction for matching display and superposition of multiple images are discussed. General computing and system hardware requirements are also described.

A. GEOMETRICAL DISTORTIONS

In all imaging systems, a square coordinate grid placed in front of the sensor does not appear square on display. The resulting effect is called geometrical nonlinearity or geometrical coordinate distortion. A simulation of the effect can be achieved by plotting a square grid on a flexible surface (say a rubber sheet) and then stretching it to destroy the rectilinear pattern. Geometrical distortion usually affects only the position and not the intensity of pixels, although in scanning systems the two effects are interrelated because the density of scan lines in a given region influences the apparent brightness. Regardless of whether a human observer or a measurement system ultimately uses the image information, some correction of these nonlinearities is generally necessary. If a number of different sensors view the same general scene and are to be superimposed for viewing (as in multispectral imaging) it is important that the effects of different relative distortions in all systems be corrected. Typical sources of geometrical distortions in imaging systems include: (a) nonlinearities in the sensor and scanning electronics; (b) aberrations in the imaging optics, such as pincushion and barrel distortion; and (c) differences in the relative orientation between multiple sensors.

The objective of this section is to develop procedures that correct distorted images for display in real time. When the output of many sensors are to be superimposed, the correction must be independently accomplished for all prior to display, and it is assumed that similar procedures will be applied to each sensor. The distortion is modeled as memoryless mapping of object scene points to display pixels, with no inherent smearing or averaging.

The distortion is fixed in time, or at least slowly varying, so that calibration of the correction system is not required during use.

Assume that the geometrically ideal image intensity is given by $f(x,y)$, where (x,y) are spatial variables in a rectilinear coordinate system defined over the entire display field. The sensor measures this ideal image intensity, where it becomes the distorted image intensity $g(u,v)$ at position (u,v) in the distorted coordinate system over the sensor field of view. The distortion relation between systems is given parametrically by

$$x = \alpha(u,v) \tag{1a}$$

$$y = \beta(u,v) \tag{1b}$$

Substitution of Eq. (1) in $f(x,y)$ and equating the intensity measurement gives the relation

$$f(x,y) = f[\alpha(u,v), \beta(u,v)] = g(u,v) \tag{2}$$

between f and g. The distortion given by Eq. (1) may be nonlinear functions of (u,v) but must be one-to-one mappings of points from one coordinate system to another as depicted in Figure 6. If the distortion is a linear function of the coordinates, then straight lines are transformed to straight lines and the transformation reduces to a combination of magnification, rotation, and translation. With these given properties of Eq. (1), the system may be inverted and solved to produce

$$u = \phi(x,y) \tag{3a}$$

26
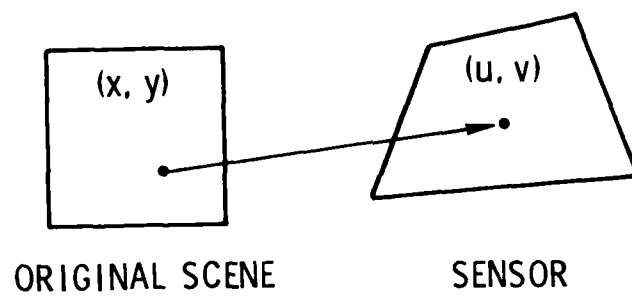
Figure 6.   Sensor Distortion
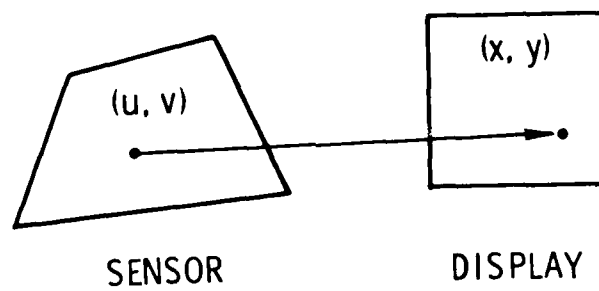
Figure 7. Ideal Correction

$$v = \psi(x,y) \qquad \qquad (3b)$$

which is the ideal inverse distortion. The optimum distortion correction system simply takes $g(u,v)$ from the sensor and substitutes in Eq. (3) to give

$$g(u,v) = g[\phi(x,y), \psi(x,y)] = \hat{f}(x,y) \qquad \qquad (4)$$

where $\hat{f}(x,y)$ is the corrected estimate. This operation is shown in Figure 7 and is the goal of all the correction systems proposed here.

The geometrical correction to recover $\hat{f}(x,y)$ from $g(u,v)$ is accomplished by first constructing the distortion model of Eq. (3) and then placing the pixel value $g(u,v)$ in the correct position (x,y) to give the estimate of the ideal image $\hat{f}(x,y)$. The second process is called "resampling."

In a scanned display system, the spacing of the scan lines and scanning speed influences the brightness observed by the viewer. In this case, Eq. (2) describing the degradation must be modified from a simple point movement by adding a multiplicative term. The requirement is that the power collected by the imaging system which is radiated from a particular spatial region of the object must be conserved at any time instant. Thus, the power radiated by a small region dxdy around object point (x,y) is measured as

$$f(x,y) \, dxdy = g(u,v) \, dudv \qquad \qquad (5)$$

in the distorted coordinates. Using the distortion relations Eq. (1), the elemental areas dudv and dxdy are related by

$$dxdy = J(u,v) \, dudv \qquad \qquad (6)$$

where

$$J(u,v) = \begin{vmatrix} \dfrac{\partial \alpha}{\partial u} & \dfrac{\partial \alpha}{\partial v} \\[2ex] \dfrac{\partial \beta}{\partial u} & \dfrac{\partial \beta}{\partial v} \end{vmatrix} \qquad \qquad (7)$$

28

is a Jacobian determinant. Substituting into Eq. (7) gives

$$g(u,v) = J(u,v) \, f[\alpha(u,v), \, \beta(u,v)] \tag{8}$$

as the distorted image. This expression differs from Eq. (4) found previously by the multiplicative factor $J(u,v)$. The effect of $J(u,v)$ is a multiplicative gain which varies with position, and it may be included with other intensity nonlinearities of the system.

Figure 8 is a block diagram of a distortion correction and resampling system. In the next few sections we describe major subsystems.

B.   CONSTRUCTION OF DISTORTION MODEL

To find the inverse distortion model of Eq. (3), pairs of control points or landmarks in both the reference and sensor coodinate systems must be found.

Figure 9 shows labeled pairs of points (A-A´), (B-B´), etc., in the sensor and corrected sensor coordinates. We assume that these match points are available from correlation, sequential similarity detection, symbolic matching, or hybrid algorithms that are described later in this report. From these data, a model of the distortion can be obtained.

An analytical model of the distortion correction can be obtained from mapping polynomials in (x,y) of degree N having the form

$$u = \phi(x,y) = \sum_{p=0}^{N} \sum_{q=0}^{N-P} a_{pq} \, x^p y^q \tag{9a}$$

$$v = \psi(x,y) = \sum_{p=0}^{N} \sum_{q=0}^{N-P} b_{pq} \, x^p y^q \tag{9b}$$

where a_{pq} and b_{pq} are the constant polynomial coefficients [4], [6], [7]. Special cases of Eq. (9) include the linear or affine model

$$u = a_{10}x + a_{01}y + a_{00} \tag{10a}$$

29
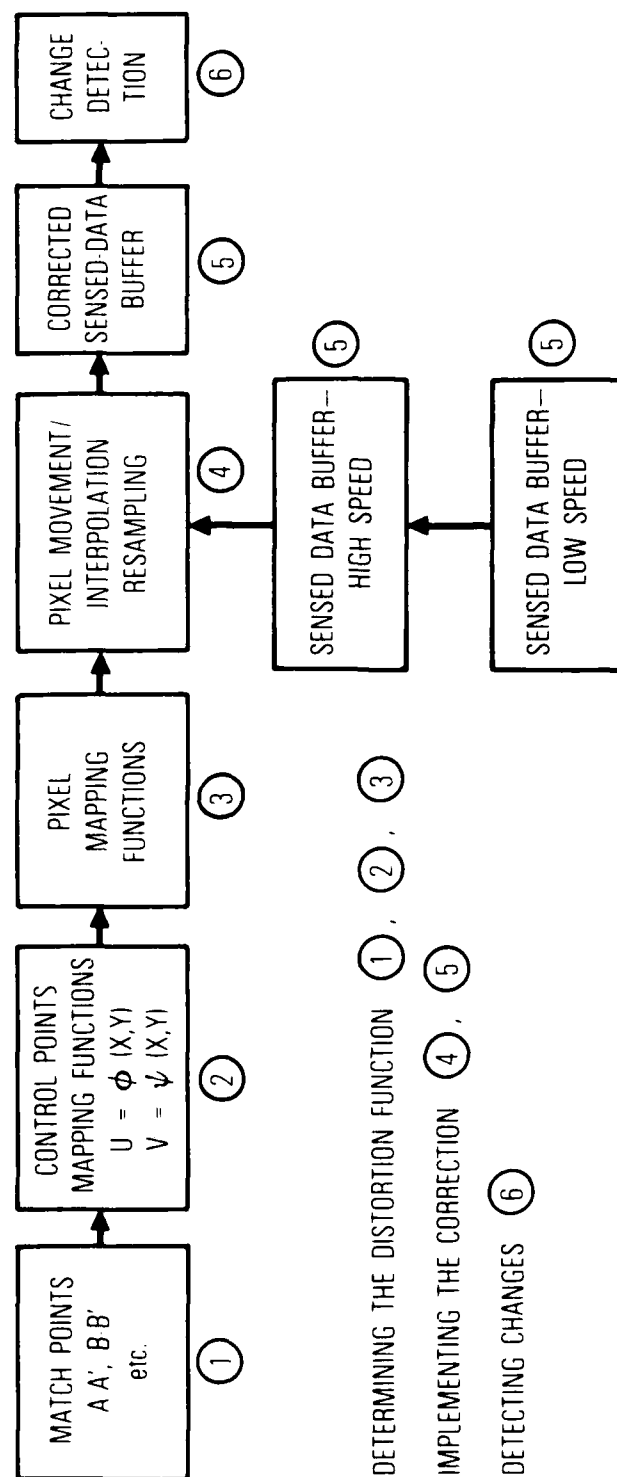
Figure 8. System Block Diagram

30
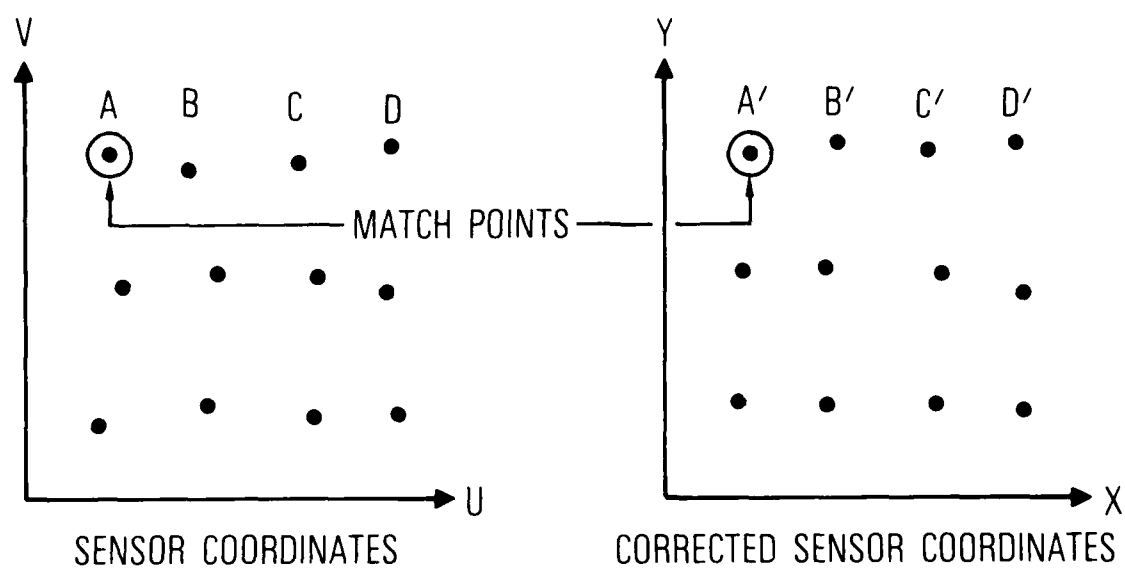
Figure 9. Labeled Pairs of Match Points

$$v = b_{10}x + b_{01}y + b_{00} \qquad (10b)$$

and the bilinear distortion model

$$u = a_{11}xy + a_{10}x + a_{01}y + a_{00} \qquad (11a)$$

$$v = b_{11}xy + b_{10}x + b_{01}y + b_{00} \qquad (11b)$$

Many local distortions in an image are accurately modeled by linear or bilinear equations. For many practical cases involving the human observer in real time or when the distortion is not severe, a second degree (N=2) approximation is probably sufficient. Lillestrand [7] describes the error as a function of increasing polynomial terms and shows that little is gained by N greater than 2 or 3. However, for large areas and more severe distortions, higher order polynomials are necessary. Alternatively, a large image may be divided into a number of smaller patches to which a linear or bilinear equation is applied. Figure 10 shows how individual pixel locations are found by bilinear interpolation on a mesh of points obtained from mapping polynomials.

Finding the coefficients in Eq. (9) involves fitting two dimensional functions to a set of measured values. Various estimation techniques can be used [8], [9], most of which provide a minimum mean-squared error (MMSE) fit. Two approaches to the fitting are described here.

Direct modeling is the first technique. It requires prior knowledge about the position of control points in the sensed and reference images. An alternative is indirec. modeling, in which a structural model of distortion is derived from knowledge of the imaging process. For example, it is possible to infer a distortion model from knowledge of the angle of elevation and other parameters. The parameters in the model may be determined by logging data from the imaging device, for example, the camera parameters (focal length) and the vehicle parameters (x,y, and z coordinates in three-dimensional space, and roll, pitch, and yaw). This approach is common in interpreting aerial photographs.
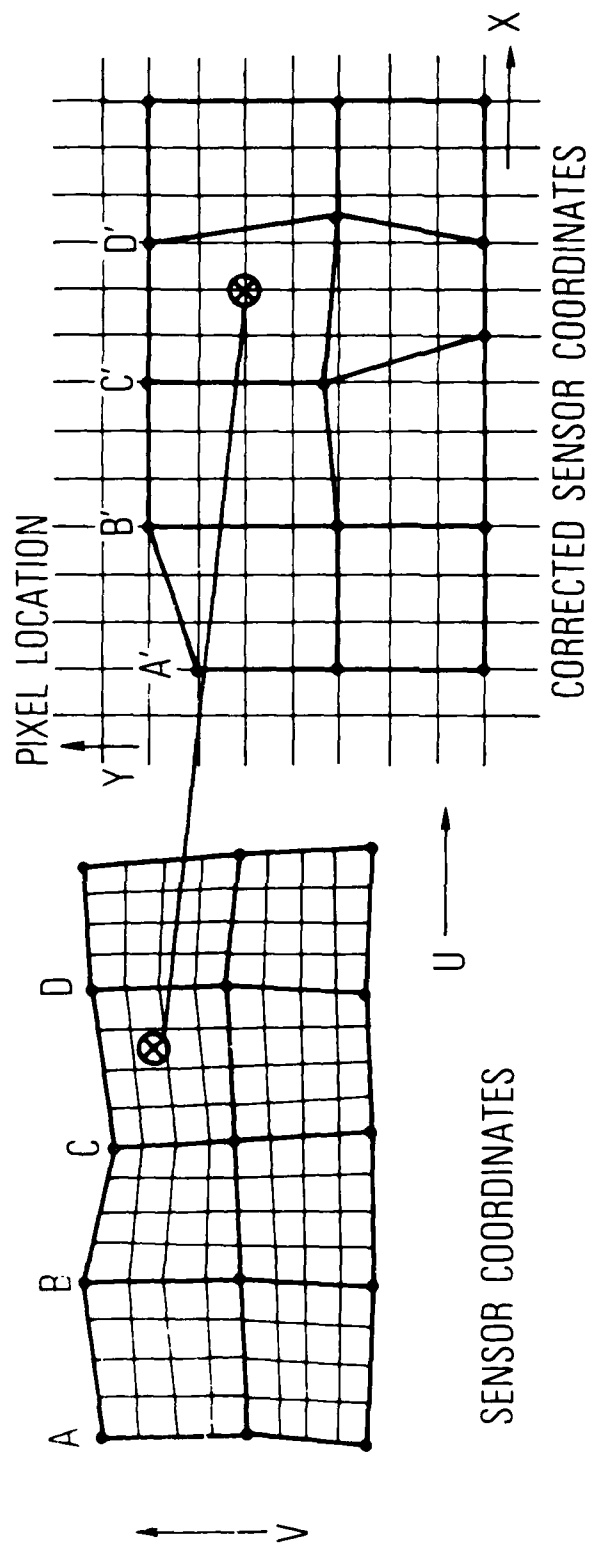
Figure 10. Labeled Pairs of Match Points for Determining The Distortion Functions

33

MMSE fitting expresses the $\phi(x,y)$ and $\psi(x,y)$ surfaces by polynomials whose squared distance from the true surface is a minimum. To obtain the coefficients, control point pairs are identified in sensed and reference images. R control point pairs are selected, and their values of $u = \phi(x,y)$ and $v = \psi(x,y)$ are recorded. For a second degree (N=2) approximation to this distortion, there are six coefficients to determine, and the measured data for (u,v) are arranged in the form

$$
R \begin{bmatrix} u^1 \\ u^2 \\ u^3 \\ \cdot \\ \cdot \\ u^R \end{bmatrix} = R \begin{bmatrix} 1 & x' & y' & x^2 & y^2 & xy \\ & & & \cdot \\ & & & \cdot \\ & & & \cdot \\ & & & \cdot \\ & & & \cdot \end{bmatrix} \begin{bmatrix} a_{00} \\ a_{10} \\ a_{01} \\ a_{20} \\ a_{02} \\ a_{11} \end{bmatrix} 6 \tag{12}
$$

Equation (12) can be expressed as the vector equation

$$
\underline{u} = D\underline{a} \tag{13}
$$

where u is an R-vector of measured output points ($R \geqslant 6$), D is the matrix of input calibration points, and $\underline{a}$ is the coefficient vector. Using MMSE estimation theory, the best estimate for $\underline{a}$ is

$$
\hat{\underline{a}} = (D^T D)^{-1} D^T \underline{u} \tag{14}
$$

where T and -1 denote transpose and inverse, respectively. The data for $\underline{v}$ are taken at the same time and used to find $\hat{\underline{b}}$ for the polynomial of Eq. (9). If greater accuracy is required for measurement purposes and N = 2 is unsatisfactory, more terms in the expansion can be used and the size of D enlarged. For

multiple sensors which are superimposed, the entire procedure is repeated for each. It is also possible to improve the approximation over the polynomials of Eq. (9) with the same number of terms in many physical systems [9].

C. DISTORTION CORRECTION SUBSYSTEMS

The subsystems labeled 4 and 5 in Figure 8 perform the actual correction based on the pixel correction functions derived in the previous section. The system consists of sensed data buffers analyzed in a speed hierarchy as shown. The low-speed data buffer may be a disc, tape, or mass storage system that transfers data to a higher speed but lower capacity system. The high-speed data buffer is generally random access memory (RAM) in a computer.

The pixel movement/interpolation system performs a correction by stepping through the discrete output (x,y) locations and finding the corresponding distorted locations (u,v). The polynomial mappings can either be precomputed and stored in a separate lookup table, or they can be computed on the fly from the polynomials.

When the distorted location (u,v) is found, the intensity value and local neighbors stored there are used to compute a geometrically corrected value that is transferred to the output buffer. The general process is called resampling and is discussed in detail in Section V. The simplest form of resampling is to do no interpolation – the nearest neighbor pixel value to the location specified by the polynomials is simply moved to the output buffer. Other methods of interpolation are given in Section V.

In general, the sensed data buffers need to store only as many pixels as needed to fill one line of the corrected data buffer. Other important considerations in hardware implementation of the distortion are the number of image pixels, speed of implementation, and the maximum amount of gross rotation distortion between sensed and reference images. In general, the sensed image buffer should be as large as possible to reduce accesses to slower-speed mass storage devices such as discs. Large sensed images may not entirely fit in a high speed buffer, so that many disc accesses may be needed for large distortions. A 90-deg rotation of sensed image is the worst possible case because it effectively requires a transpose of a large array, or

35

equivalently, each corrected pixel comes from a different line of the sensed image. For small distortions, the high speed buffer can be much smaller because fewer lines of the sensed image are needed to generate one corrected line. Sophisticated data base organization, parallel processors, and parallel disc access hardware may be effectively used in speeding up the correction process.

IV. RECTIFICATION AND CHANGE DETECTION ALGORITHMS

Three major categories of rectification algorithms have emerged from the study.

- Signal-processing-based (SP)

- Artificial-intelligence-based (AI)

- Hybrid techniques

The signal-processing-based algorithms use various correlation methods to find the best match between reference map and sensed image. The AI-based algorithms compare symbolic representations of features extracted from both images. Hybrid techniques combine approaches in an effort to make the best use of both.

In this section, various image matching algorithms for multisensor environments are studied and analyzed in detail. Change detection algorithms are also reviewed.

A. TYPES OF ALGORITHMS

Two basic types of matching procedures exist: signal processing or correlation-based techniques; and artificial intelligence or symbolic-based techniques. More recently, hybrid techniques have been developed that attempt to make the best use of both procedures (see Figure 11). The signal processing techniques work by correlating intensity values of original or enhanced portions of the sensed images against the reference. The best match based on a match quality measure is then recorded. There are a number of ways to perform the correlation, and a fast algorithm known as sequential similarity detection (SSDA) offers a speed improvement by a factor of 100 over conventional correlation. The artificial intelligence techniques compare symbolic representations of features extracted from both reference and sensed images. These features can be edges, lines, vertices of line intersections, shapes, etc. Given a distance function or other relative match quality measure, graph matching or searching techniques such as relaxation labeling are used to

37
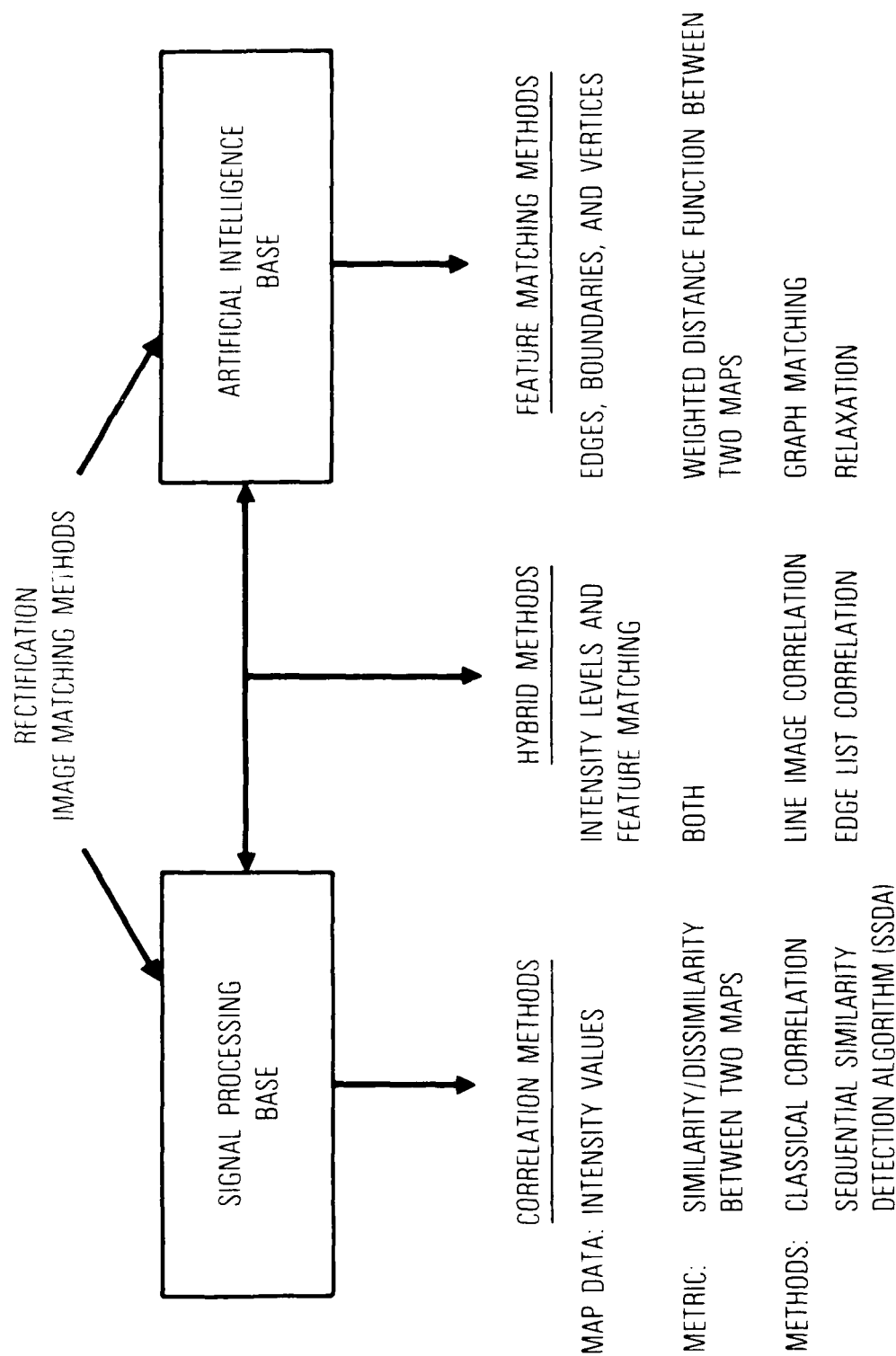
Figure 11. Categories of Rectification Algorithms

RECTIFICATION
IMAGE MATCHING METHODS

ARTIFICIAL INTELLIGENCE BASE

SIGNAL PROCESSING BASE

CORRELATION METHODS

MAP DATA: INTENSITY VALUES

METRIC: SIMILARITY/DISSIMILARITY BETWEEN TWO MAPS

METHODS: CLASSICAL CORRELATION
SEQUENTIAL SIMILARITY DETECTION ALGORITHM (SSDA)

HYBRID METHODS

INTENSITY LEVELS AND FEATURE MATCHING

BOTH

LINE IMAGE CORRELATION
EDGE LIST CORRELATION

FEATURE MATCHING METHODS

EDGES, BOUNDARIES, AND VERTICES

WEIGHTED DISTANCE FUNCTION BETWEEN TWO MAPS

GRAPH MATCHING
RELAXATION

compare reference and sensed symbolic data sets. The symbolic data have a much lower dimensionality than pixel-based signal processing data, thus computations should be reduced for symbolic matching. One additional tradeoff between the techniques concerns noise resistance. Correlation techniques provide inherent noise suppression and can find good matches with significant amounts of image noise if the relative magnification, rotation, and distortion differences are not great. Symbolic matching strongly relies on good, noise-free feature extraction. With noisy edges, lines, vertices, etc., symbolic techniques will fail, thus good preprocessing for noise suppression and robust, noise-resistant feature extract is essential for symbolic matching. Hybrid techniques combine both approaches to make the best use of both. Tables 2 and 3 summarize this result for various types of sensors under study and for the different error categories discussed in section II.

B.   SIGNAL-PROCESSING-BASED ALGORITHMS

The standard signal processing technique for registering images is to form a correlation measure between them as a function of translational shifts and find the location that gives the maximum correlation value. Several references discuss this problem [10,12], and the book by Pratt [13] summarizes the results.

The simplest form of a two-dimensional correlation measure is given by

$$R(m,n) = \frac{\sum\limits_{j=1}^{J} \sum\limits_{k=1}^{J} F_1(j,k)\, F_2(j-m, k-n)}{\left[\sum\limits_{j=1}^{J} \sum\limits_{k=1}^{K} F_1^2(j,k)\right]^{1/2} \left[\sum\limits_{j=1}^{J} \sum\limits_{k=1}^{K} F_2^2(j-m, k-n)\right]^{1/2}} \quad (15)$$

where $F_1(j,k)$ and $F_2(j,k)$ are two discrete images to be registered, and (j,k) are indices in a $J \times K$ pixel window area W that is located within an $M \times N$ point search area S. Figure 12 shows the search and window areas. In general, the correlation function is computed for all $(M-J+1)\,(N-K+1)$ possible

39

Table 2. Sensor-Dependent Rectification Methods

SENSOR	TYPE	LOW SNR	MODERATE SNR	HIGH SNR
OPTICAL/NEAR IR	P,A	CORRELATION	HYBRID	FEATURE MATCHING
MIDDLE IR	P	HYBRID	HYBRID	FEATURE MATCHING
	A	CORRELATION	HYBRID	FEATURE MATCHING
THERMAL IR	P	HYBRID	HYBRID	FEATURE MATCHING
	A	CORRELATION	HYBRID	FEATURE MATCHING
MICROWAVE	P	CORRELATION	HYBRID	FEATURE MATCHING
SAR	A	1-D CORRELATION 2-D HYBRID	HYBRID	(not adequate SNR)

P = PASSIVE SENSORS
A = ACTIVE SENSORS

40

Table 3. Algorithm Error Analysis

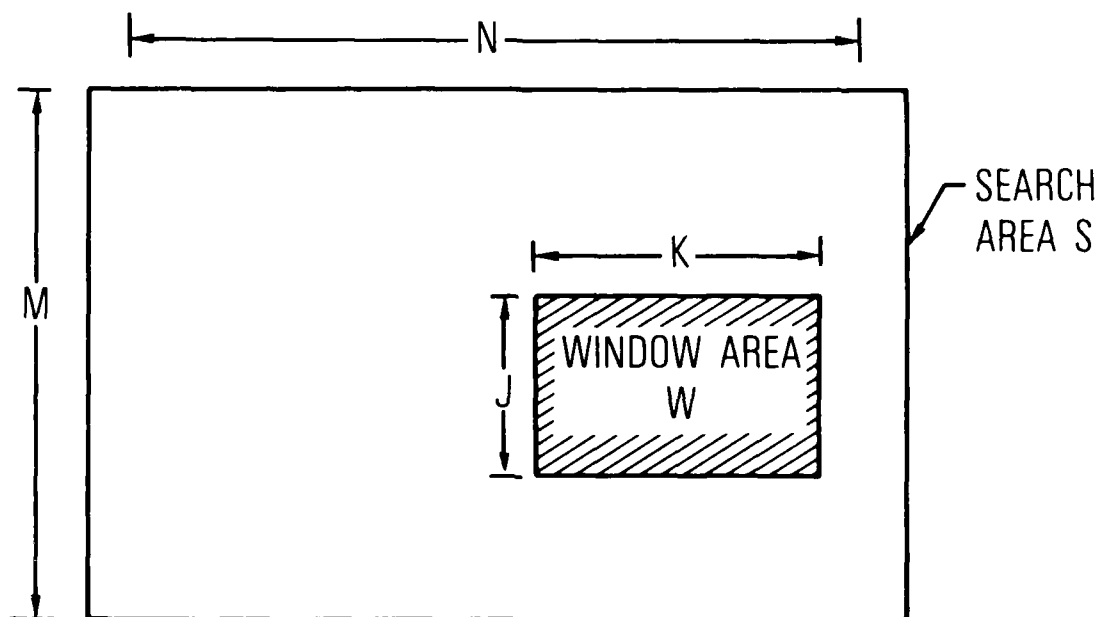|	ERROR CATEGORY			
ALGORITHM	GLOBAL (Geometric, radiometric)	REGIONAL (Contrast reversal)	LOCAL (Noise)	NONSTRUCTURED (Others)
CORRELATION	MEDIUM	POOR	GOOD	GOOD
FEATURE MATCHING	MEDIUM	GOOD	POOR	POOR
HYBRID	GOOD	GOOD	MEDIUM	GOOD

Figure 12. Correlation Search and Window Areas

translations of the window area within the search area to find its maximum value and the displacement that gives the best match.

One possible problem with the correlation technique is that the correlation function may be very broad, making detection of the peak difficult. This will particularly happen if the search and window images contain large uniform regions with very few details. Another problem is that differences in scale size, geometric distortion, rotation, and relative intensity between the two images will make registration difficult and effectively suppress the correlation peak. Pratt [13] has described some techniques for avoiding the first problem. They consist of prefiltering the window and search areas with a Laplacian spatial high-pass filter that effectively performs edge enhancement.

Another difficulty with the correlation method of image registration is the large amount of computation needed. In Eq. (15) the correlation measure R_s (m,n) must be computed for all (m,n) before the maximum can be selected, and the amount of computing is the same for all degrees of misregistration.

To overcome some of these problems, a class of algorithms known as sequential similarity detection (SSD) has been developed by Barnea and Silverman [14]. These algorithms provide a test for misregistration with fewer computations.

The basic form of the algorithm is to compute an error measure

$$\epsilon \ (m,n) = \sum_j \sum_k \ |F_1 \ (j,k) - F_2 \ (j{-}m, \ k{-}n)| \qquad (16)$$

where the sums are taken over the window area and F_1 and F_2 are the window and search functions, respectively, as before. However, the sum is <u>not</u> taken over a regular scan indexing of (j,k). Instead, the absolute value of the difference in Eq. (16) is accumulated for randomly selected points in the window area. If the accumulated error exceeds a fixed threshold before all J × K points in the window area are examined, then it is assumed that a particular

43

shift (m,n) is a poor candidate for matching, and another shift of the window is checked. If the error grows slowly, then the number of points examined when the threshold is finally exceeded is recorded and used as a rating of a particular shift (m,n). When all possible shifts have been examined, the window with the largest rating is chosen as best. The highest possible rating is equal to the number of window points $J \times K$. In this way, shifts that are grossly incorrect are discarded rapidly after only a few computations.

The SSD algorithm can also be combined in a hybrid approach as a preprocessor for correlation registration. The SSD algorithm can be used to discard gross misregistration, while a correlation algorithm can be used for the final refinement. A reduction in computations by a factor of 100 over correlation has been experimentally observed using SSD techniques.

C. ARTIFICIAL-INTELLIGENCE-BASED ALGORITHMS

As outlined earlier, feature matching algorithms do not directly use intensity data. Instead, they use scene features such as edges, boundaries, and line vertices. The first stage of processing generally extracts these features. Then distance functions between sensed and reference image features are defined and a search for the best match is made. The search techniques can include graph matching, and nonlinear or linear optimization. Some examples of scene matching techniques are discussed in detail here.

There are two major types of artificial intelligence (AI)-based algorithms for image matching that require little or no a priori control point information. These techniques are: clustering features and feature groups; and structural/symbolic matching.

The clustering approach begins with features extracted from both reference and sensed images. These features can be intensity itself, edges, texture, etc. No labeled control points are present in the two images. The general algorithm provides a reward for region correspondence based on the clustering of the joint histogram of features in the two images. The algorithm tries to measure the correspondence of features of each type in the two images and finds the rotation, translation, and scaling needed to create a

44

correspondence. It increments the cluster model by one unit at each such angle, x-y coordinate, or scaling parameter, and groups values corresponding to the identification of two features with one another. This approach can immediately follow front-end feature extraction. Basic references are [15-17]. Reference [18] discusses sequential feature detection, which may be useful in speeding up these routines.

Structural and symbolic matching is to date a research-level algorithm process involving automatic interpretation, but it is principally applied to partially specified scenes [19] and structure interpretation from image boundaries [20]. A data structure system has been created as part of the ACRONYM [21] model-based vision system involving five levels of graphs: "context," "object," "observability," "interpretation," and "picture" [19]. Also, much work has been done using linear features [22].

Additional detailed work on scene matching, performed by Hughes Research Laboratories [23,24], has developed scene matching systems that extract line and vertex features derived from the scene. Feature weighting, based on matchpoint location and model feature content, is used to define geometrical transformations between reference and sensed models that lead to highly accurate matchpoint location. An important part of this work is the use of data structures for regions, lines, vertices, and connected groups that contain parameters and links to other data elements. The technique is experimentally highly tolerant to differences in scene contrast, scale, and orientation differences. More details of these algorithms in their specific application to SAR image matching are given in section VI.

D. CHANGE DETECTION ALGORITHMS

Once the sensed and reference images are rectified and spatially registered, both signal processing and symbolic approaches are available for change detection, in a manner similar to that used to obtain pairs of match points (see Figure 13). Any change detection method must contend with differences in illumination, sensor, wavelength, and surface conditions [6,7]. Some of these effects can be compensated for by a priori knowledge. Signal

45

REFERENCE IMAGE
RECTIFIED SENSED IMAGE

ARTIFICIAL INTELLIGENCE APPROACH

SYMBOLIC MATCHING

HYBRID APPROACH

SIGNAL PROCESSING APPROACH

DIFFERENCING/CORRELATION

VISIBLE, IR, SAR

- SEGMENT IMAGE
- EXTRACT SYMBOLIC DESCRIPTION
- FIND SYMBOLIC DIFFERENCES

- KNOWLEDGE REPRESENTATION
- SEMANTIC INFORMATION

VISIBLE, IR

- FIRST-ORDER PROBABILITY DENSITY (histogram) OPERATIONS ARE ADEQUATE
- PIXEL DIFFERENCING

SAR

- SPECKLE IS A PROBLEM
- USE DIFFERENCES OF HIGHER-ORDER SPATIAL STATISTICS (texture)

Figure 13. Change Detection Between Geometrically Rectified Scenes

46

processing approaches for registered visible and IR images include pixel differencing, although speckle and other texture artifacts in SAR images may cause problems. Symbolic techniques for change detection involve segmenting the images into regions or shapes with similar feature properties, and extracting symbolic descriptions of these regions. The symbolic descriptions may be edges, lines, shapes, or other higher-level visual features. These symbolic descriptions are compared by graph matching, searching, etc., similar to the general techniques described for finding match points. This type of change detection allows additional knowledge, such as contextual relationships and semantics, to be included in the change detection process. Also, hybrid approaches that combine signal processing and symbolic processing have been studied. More investigation into techniques of change detection is needed [15,16].

V. RESAMPLING PROCESS

In the process of registration and rectification of remotely sensed data, a problem arises as a result of nonuniform spacing of the input pixel values in both along-scan and across-scan directions. This distortion of a regular grid and pixel points is a result of implementation of geometric and radiometric corrections on the image data. It then becomes necessary to evaluate new data values of the sample in order to achieve a regular rectangular grid of output pixels with the desired number of lines and sample/lines for the purpose of registration. This process is called "resampling."

In this section, an overview of the resampling process as it relates to registration and rectification of onboard sensor imagery is discussed. Various one- and two-dimensional resampling techniques are reviewed and compared.

A. BACKGROUND

Resampling involves constructing an ideal image by determining for each pixel (x,y) the corresponding pixel in the distorted image. The intensity value of the pixel in the distorted image is then copied into its undistorted position in the ideal image. Unfortunately, a pixel position (i,j) in an ideal image will usually not map to an integer coordinate (m,n) - the exact pixel position whose value is sampled in the distorted image - but to a point (u,v) between pixel locations (see Figure 14). How, then, is the value at (u,v) - the value to be copies into pixel (i,j) - to be determined? There are two common solutions to this problem. One is to copy the value of the nearest neighbor to (u,v) into the ideal image. The other is to interpolate a value based on the values of pixels in a window around (u,v).

During the past decade, a great deal of research was carried out regarding the application of digital interpolation techniques to remotely sensed digital images [25-28].

Perfect image reconstruction is possible with a number of interpolating kernels (reconstruction filters) for band-limited image samples with a proper
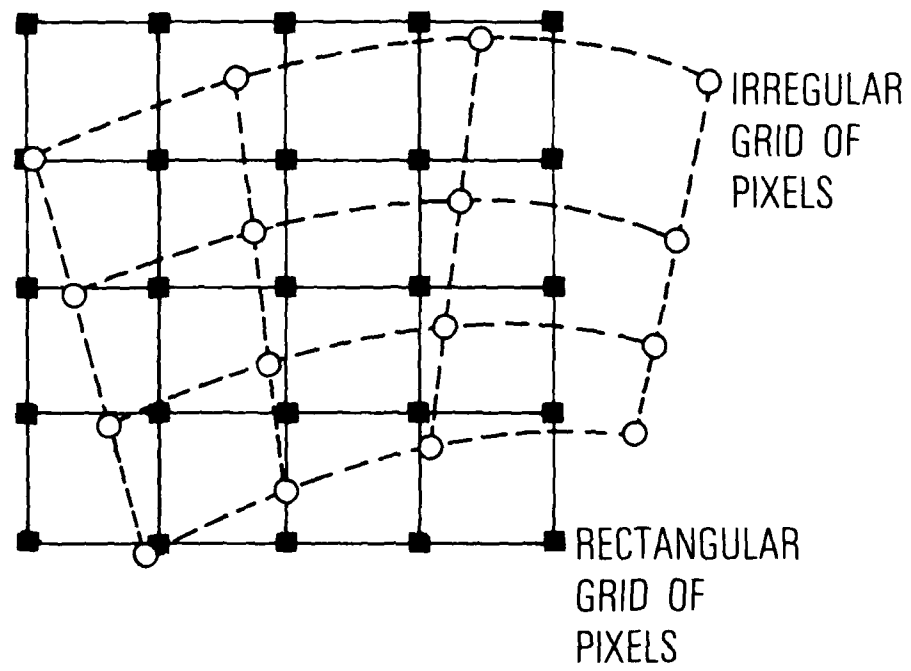
49

IRREGULAR
GRID OF
PIXELS

RECTANGULAR
GRID OF
PIXELS

Figure 14. Resampling Process

50

sampling period. For example, a sinc function can be used as an interpolating kernel for exact reconstruction of an infinite number of sufficiently close samples of a band-limited image [35]. In practice, however, because of limitation in computation time and storage, it is often difficult or impractical to produce exact reconstruction of an imaging system and, instead, simple approximating techniques are used.

B. RESAMPLING TECHNIQUES

Three approximating techniques are commonly used in resampling of one- or two-dimensional data: nearest-neighbor, bilinear interpolation, and cubic convolution (spline interpolation).

Figure 15 shows how pixel values are determined for a location (X) in between pixels for the above three techniques. In this figure, pixels are presented by dots, and lines connecting pixels show the pixels used in interpolation to determine an image data value at the location presented by deltas. Lines connecting the deltas show another interpolation process required to find the data value at location X.

For nearest neighbor resampling, the data value of the pixel closest to the resampled pixel (location X) is chosen for the result of the interpolation operation. The interpolation kernel is linear and is shown in Figure 16. This kernel produces position (horizontal and vertical) errors throughout the operation, as much as ±0.5 pixel spacing, which results in rapidly changing contours (jitters) in the region of high contrast [25,26].

The bilinear interpolation kernel shown in Figure 16 requires a bilinear combination of four pixel values closest to the desired location X [Figure 15(b)]. The smoothing effects of bilinear interpolation cause some image degradation in the form of edge smoothing and loss of maxima/minima structure [26-28].

The cubic convolution process, which is an approximation of the sinc function by cubic polynomials with a kernel shown in Figure 16, requires the values in a grid of 4 × 4 pixels about the desired resample pixel location X

51

NEAREST-NEIGHBOR
INTERPOLATION
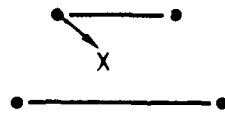
BILINEAR
INTERPOLATION
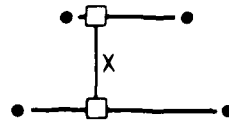
CUBIC
CONVOLUTION
PROCESS
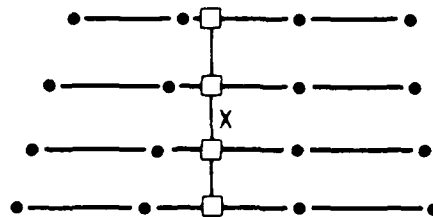
- PIXEL LOCATION
- □ INTERPOLATION
  VALUE LOCATION

Figure 15.   Interpolation to Desired Location X

52
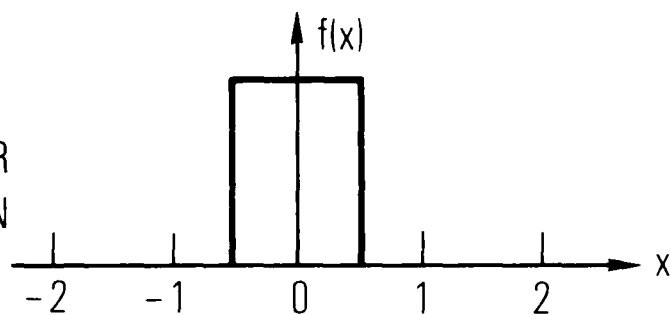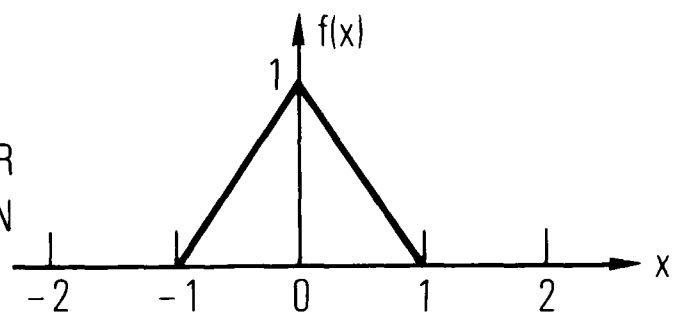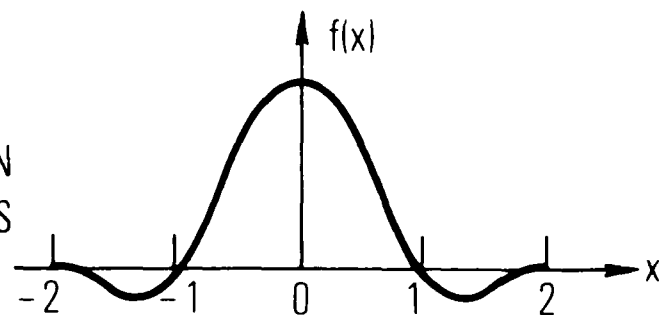
Figure 16. One-Dimensional Interpolation Kernels

53

[Figure 15(c)]. This approach [27] in the earlier reports was shown to give better results, even in comparison with sinx/x truncated at 10 pixels.

C. INTERPOLATION PROCESS

Once the match points for the distortion are computed, it is necessary to resample the irregularly spaced data at coordinates (u,v) so as to produce output image data at coordinates (x,y) defined on a regular grid of pixels. The resampled image data are, in general, computed by an interpolation procedure.

$$g(x,y) = \sum_{u,v} f(u,v) \, K(x-u, \, y-u)$$

where

K = interpolation kernel

f = available raw data values

g = resampled data values

Note that for integer values of x,y the corresponding image coordinates u = x + δx and v = y + δy are noninteger values, where δx, δy are image distortion approximations.

Although several two-dimensional interpolation kernels for regularly and irregularly spaced data are available [12, 32, 33], in practice, the two-dimensional kernel K is considered as a separable kernel

$$K(x-u, \, y-u) = k(x-u) \, h(y-u)$$

and the resampling process is implemented as two one-dimensional interpolations: first in the direction of raw data scan lines, and then in the orthogonal direction.

Note that the ideal interpolation kernel for band-limiting data is of the form

$$K(x-u, y-u) = C \frac{\sin \pi (x-u) \sin \pi (y-u)}{\tau^2 (x-u) (y-u)}$$

However, this function has significant magnitude until very high $|x,u|$ and $|y-v|$ and, thus, the summation terms for each interpolation tend to be very large.

In one dimension, the simplest interpolating kernel is the pulse function, which results in nearest neighbor resampling. A triangle function provides a bilinear interpolating kernel (Figure 16). The cubic convolution kernel is described in the next section; its smooth curve actually coincides with the original data values.

D. CUBIC CONVOLUTION INTERPOLATION

Cubic convolution interpolation is an approximation to the resampling process by fitting a piecewise polynomial to the sinc function through interpolation while imposing certain constraints [26]. The contribution of a spline kernel to the approximation method is twofold: (a) reduction of the summation term in the ideal interpolation from an infinite number to a summation over four input sample pixels; and (b) optimization in terms of zero mean error and minimum error variance.

Simon [28] was the first to introduce the cubic convolution interpolation using splines and formulating the resampling problem as a constrained linear estimation problem with suitable image models and optimization criteria. In this paper the interpolation kernel is called "cubic convolution," but the piecewise cubic polynomials used for the approximation are not simple splines by nature, since they do not follow the continuity criteria that are specific to spline functions.

A spline function of order k is defined to be a piecewise polynomial function of order k on some interval with k-2 continuous derivatives [29,30]. In other words, a spline function is a piecewise polynomial function that is as smooth as it could be without simply reducing it to a polynomial.

The one-dimensional cubic convolution kernel given by Simon is one of the form

$$k(0) = 1$$

$$k(\pm 1) = 0$$

$$k(x) = 0, \ |x| > 2$$

$$k(x) = k(-x)$$

with the constraint equation

$$k(x) + k(1 + x) + k(1 - x) + k(2 - x) = 1$$

and the further constraint of continuity of the first derivative of all knot points. The above defines a cubic polynomial with one degree of freedom, which can be taken, for example, such that the derivative of $k(x)$ at $x = 1$ be the same as that of sinc (πx). This gives the following polynomial as an approximation to a sinc function at four points:

$$k(x) = \begin{cases} 1 - 2 \ |x|^2 + |x|^3 & \text{if } 0 \leqslant |x| \leqslant 1 \\ 4 - 8 \ |x| + 5 \ |x|^2 - |x|^3 & \text{if } 1 \leqslant x \leqslant 2 \\ 0 & \text{otherwise} \end{cases}$$

which is a continuous function with a continuous first derivative at equally spaced knot points, $-1, 0, 1, 2$, but a discontinuous second derivative at ± 1. This discontinuity indicates that the above function is not a regular spline function with all its continuity properties, but is a sort of smoothness deficient spline [29-31].

E. DETAILS OF CALCULATION

In one-dimensional cubic convolution, four terms are included in the summation, i.e., only four pixel values (u_{i-1}, u_i, u_{i+1} and u_{i+2}) nearest to the desired location (X) contribute, and the interpolation equation becomes

56

$$g(x) = \sum_{i-1}^{i+2} f(u_i) \, k(x-u_i)$$

It is reasonable to assume that each array of raw image data along-scan has evenly distributed pixels with spacing $u_{i+1} - u_i = h$. Thus, the above equation reduces to

$$g(x) = f(u_{i-1}) \, k(\delta x + h) + f(u_i) \, k(\delta x)$$
$$+ f(u_{i+1}) \, k(\delta x - h) + f(u_{i+2}) \, k(\delta x - 2h)$$

where $x = u_i - \delta x$ and $h = u_{i+1} - u_i$.

A graphical presentation of the four k-values for the cubic convolution kernel described in the previous section is given in Figure 17. The summation in the above equation is also illustrated in Figure 18 where $f_i = f(u_i)$

$$k_1 = k(\delta x + t), \; k_2 = k(\delta x), \; k_3 = k(\delta x - h) \text{ and } k_4 = k(\delta x - 2)$$

and the dot represents the interpolated value $g(x)$.

In practice, several δx values are given; the corresponding k-values are precomputed and stored in a vector to be used during the resampling process.

In two-dimension, the same process can take place, except K is a matrix of 4×4 and 16 pixel values are considered for interpolation. However, as described previously, the resampling process usually takes place in two stages: first in the direction of raw data scan (along-scan line), as outlined above; and then in the orthogonal direction (across-scan lines). Across-scan line interpolation proceeds in the same manner as along-scan line, except interpolation is along columns of interpolated data (in the x-v coordinate system). Final output is usually interpolated along- and across-scan and is presented in the x-y coordinate system as a regular grid of pixels [32-34].
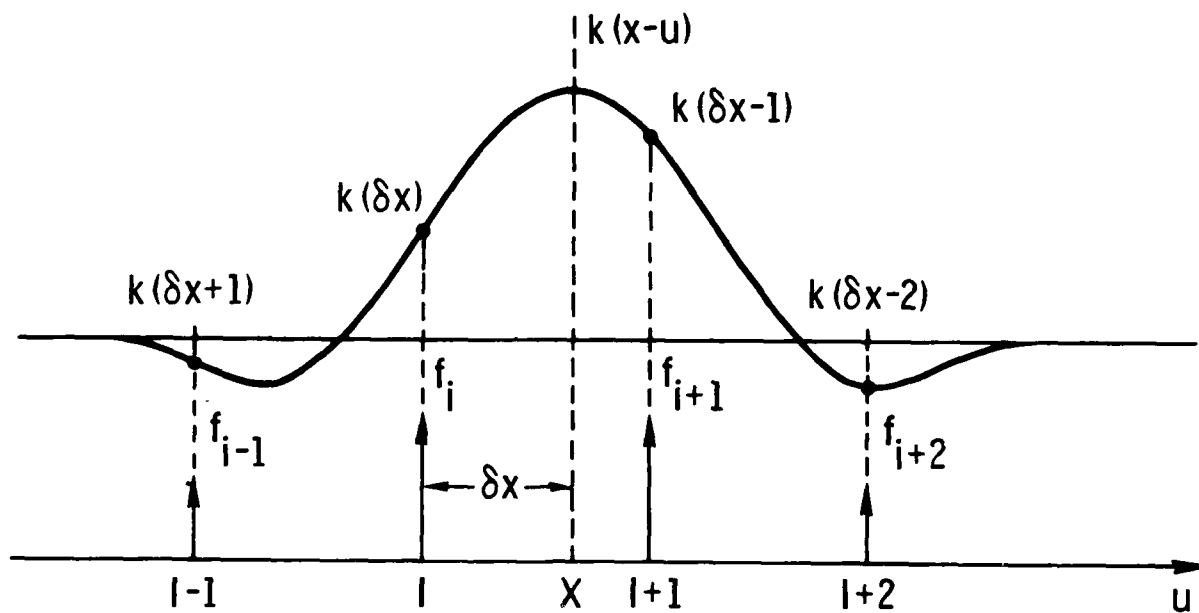
Figure 17.   Interpolation Kernel k(x) of 4-Point Cubic Convolution
(as used in the resampling process)
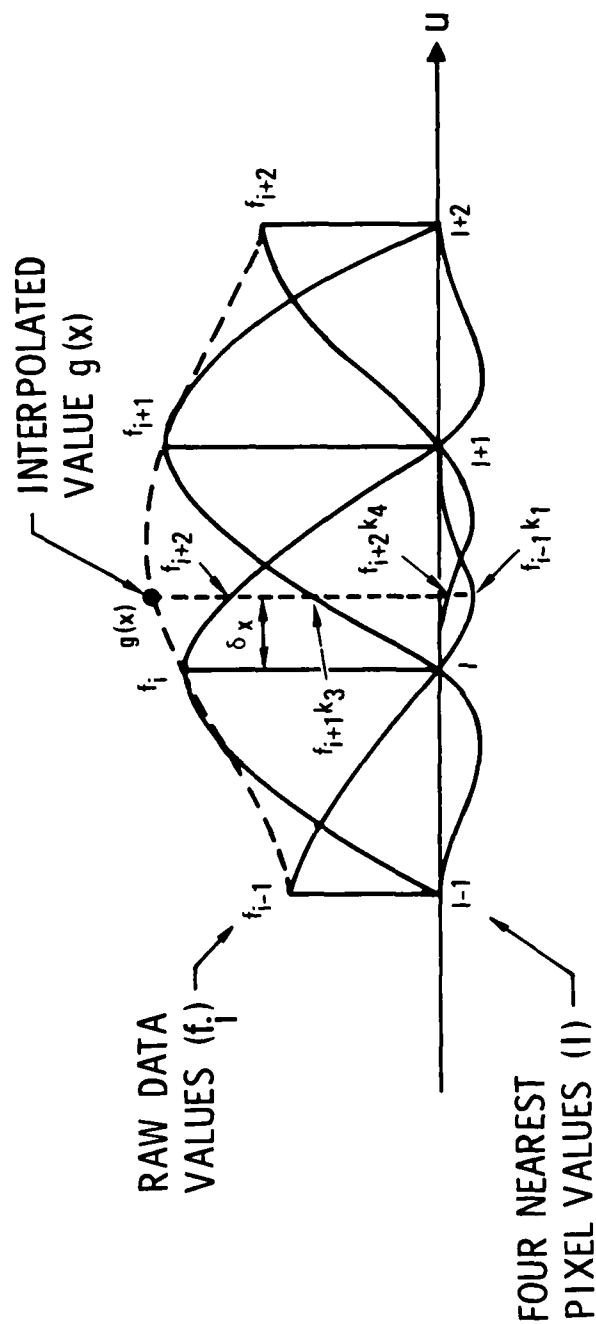
Figure 18. Interpolated Values of g(x) by Cubic Convolution. Four-point interpolation at pixel I-1, I, I+1 and I+2 with raw data values f_{i-1}, f_i, f_{i+1} and f_{i+2} for interpolated value g(x) [location of dot] is illustrated.

F.   ANALYSIS OF RESAMPLING ALGORITHMS

As pointed out previously, the most commonly used resampling technique (replication or nearest neighbor interpolation) reduces the resolution of the image, igiving it a blocked look and changing diagonal edges into staircase responses. It produces errors of the order of ±0.5 pixel spacing which, in turn, results in some sort of jitter in the high contrast regions of the imagery. The familiar bilinear interpolation technique has a smoothing effect that is pleasing to the eye but causes degradation around edges and highlights of imagery. Cubic convolution has less of a smoothing effect, but it is harder to implement.

Some resampling results [27-35] suggest advantages of nearest neighbor and bilinear interpolation over resampling by cubic convolution as a result of overshooting of data and exaggeration of peaks (valleys) occurring in the cubic convolution.

However, from the outcome of all analysis to date, it seems that the cubic convolution method is the leading method as far as computing time, statistical, and frequency-content considerations lie. On the other hand, artifacts such as ringing or other unpleasant visual effects may still be present in the final image after resampling with cubic convolution. Note that many artifacts seen in the resampled data are independent of the specific interpolation method and actually present in the original data as well. More analysis of the effect of resampling algorithms on various artifacts such as speckle, shadowing, and contrast reversals is under active study.

VI. SAR IMAGE RECTIFICATION

At present, not enough results and studies are available on the matching of SAR images to visible image or to a SAR reference map to draw conclusions from. Most of the previous work has been concentrated in the rectification and registration of visible imagery as discussed in previous sections. This section deals with specific qualities of SAR imagery which may cause serious problems in accurate image matching and investigates the feasibilities of various rectification, registration, and change detection algorithms applicable to SAR imagery.

A. BACKGROUND

The specific qualities of SAR data must be considered when a SAR image is to be registered with a visible image or when two SAR images are to be registered. SAR imagery is generally different statistically and visually from imagery obtained by visible, IR, or other wavelength sensors. SAR imagery tends to have much lower pixel-to-pixel correlation than visible imagery, and may have much greater dynamic range. For visible imagery, a dynamic range of 8 bits (256 to 1) is usually adequate; while for SAR data, the dynamic range may exceed 1000 to 1 [36-38]. Bright specular reflections (glints) from plane surfaces such as roofs and strong returns from corners of man-made structures contribute to this great dynamic range.

The coherent nature of SAR creates artifacts such as speckle and false texture in optically diffuse areas of the scene. Speckle is a granular noise arising from the random interference of wavefronts scattered from an optically rough surface [41,42]. In its most general form, speckle is signal-dependent and very objectionable visually. Speckle may create the appearance of texture in regions that appear uniformly bright at a different wavelength. The spatial scale size of the speckle is generally on the order of the limiting resolution of the coherent SAR imaging system [41-43].

Other artifacts include shadowing of surface relief features and contrast reversals in comparison to visible imagery.

Figure 19 is a simulation showing how the appearance of an aerial photograph changes with visible and SAR sensors [41]. Figure 19(a) is an example of an aerial photo at visible wavelengths. Figure 19(b) shows a digitally simulated coherent image with speckle simulated using an exact signal-dependent model. It has a signal-to-noise ratio of 2. The simulation does not include some particular SAR artifacts such as shadowing, specular reflections, and contrast inversions, but does include granular speckle noise.

Various techniques for the suppression of speckle have been investigated [41, 42, 44]. One class of techniques, which increases the signal-to-noise ratio by incoherently averaging independent looks, can be obtained by polarization, wavelength, and spatial frequency diversity. Other techniques use recursive and nonrecursive image restoration to spatially smooth speckle noise while preserving object details. Figures 19(c) and 19(d) show examples of recursive filtering applied to images with speckle. Figure 19(c) shows the image of Figure 19(b) processed by a local linear minimum mean-square error filter; Figure 19(d) shows Figure 19(b) processed by a maximum a posteriori (MAP) filter.

Very little theoretical and/or experimental work on the matching of SAR images is available [17,48,50-55]. Referring to Figures 3, 20, and 21, describing image matching methods, it is likely that signal-processing-based correlation techniques applied to SAR pixel data would be the most effective. These techniques provide some noise immunity by their inherent spatial averaging over the window area. It is probable that the usual correlation computation over windows would work well on SAR data, although it is unclear how more-sophisticated, fast algorithms such as sequential similarity detection (SSD), which do not use all data in the window, would work.

The artificial intelligence (AI)-based techniques shown in Figures 20 and 21 generally require clean, noise-free image data, and robust features such as edges, boundaries, and vertices. The AI-based matching problem then reduces to a symbolic matching of directed graphs or other relational structures using relaxation or other techniques. Hybrid techniques are useful in that they may

62

A = ORIGINAL VISIBLE IMAGE

B = SIMULATED COHERENT IMAGE
4-FRAME AVERAGE OF INDEPENDENT SPECKLE IMAGES. S/N = 2

C = IMAGE B PROCESSED BY LOCAL LINEAR MINIMUM MEAN-SQUARE
ERROR FILTER

D = IMAGE B PROCESSED BY MAP (maximum a posteriori
probability) FILTER
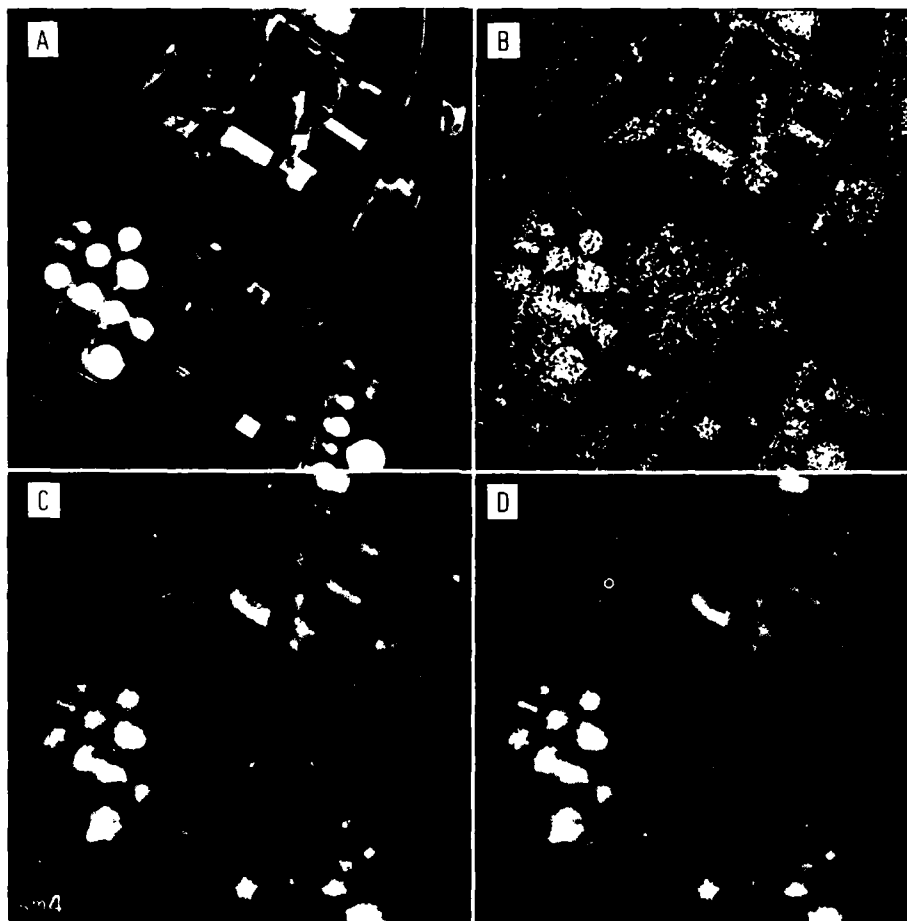
Figure 19. Visible and Synthetic SAR Images

```
┌─────────────────────┐          ┌─────────────────────┐
│    CORRELATION/     │          │     ARTIFICIAL      │
│  SIGNAL PROCESSING  │          │  INTELLIGENCE (AI)  │
└─────────────────────┘          └─────────────────────┘
```

- OPERATES ON INTENSITY VALUES

- CORRELATION

- SSDA (sequential similarity detection algorithm)

- BETTER DEVELOPED, PERHAPS MORE RELIABLE FOR SAR

- FAST ALGORITHMS POSSIBLE

- REQUIRES CLEAN, NOISE-FREE FEATURES

- USES SYMBOLIC MATCHING OF RELATIONAL STRUCTURES, GRAPH MATCHING, RELAXATION

- EASIER TO INCLUDE HIGH-LEVEL SEMANTIC KNOWLEDGE

- MORE ROBUST TO DISTORTIONS, CHANGES, CONTRAST REVERSALS

```
          ┌─────────────────────┐
          │       HYBRID        │
          └─────────────────────┘
```

- SOME AVERAGING CAN BE INCLUDED

- INTENSITY LEVELS AND FEATURE MATCHING COMBINED

Figure 20.   SAR Image Matching Techniques

• VERY LITTLE THEORY OR EXPERIMENTAL RESULTS

CORRELATION/ SIGNAL PROCESSING	ARTIFICIAL INTELLIGENCE

• BETTER DEVELOPED

• PROBABLY MORE RELIABLE

• SPATIAL AVERAGING
  PROVIDES NOISE IMMUNITY

• FAST ALGORITHMS EXIST

• LESS WELL-DEVELOPED

• APPLICABILITY TO SAR
  NOT KNOWN

• EASIER TO INCLUDE HIGHER
  LEVEL SEMANTIC KNOWLEDGE

• MORE ROBUST TO
  DISTORTIONS, CHANGES,
  CONTRAST REVERSALS

HYBRID

• COMBINES BEST OF BOTH

Figure 21. SAR Image Matching

provide some spatial averaging, but good extraction of lines, edges, and other linear features is still required.

Much research is still needed on the matching of SAR imagery. One approach is to investigate various preprocessing algorithms for noise removal, followed by matching techniques suitable for visible data (either signal processing or AI). Another approach may be to segment a SAR scene into regions of common texture and/or brightness, extract outlines of the segmented regions, and combine this with other edge/line data derived from the scene as input to a matching procedure. For AI-based symbolic matching, more a priori knowledge specific to SAR can be included. For example, in a visible image AI-based matching system, knowledge that bodies of water generally appear darker than large land masses can be used in matching. This fact may not be true in SAR imagery, and a knowledge base of relevant facts such as these can be developed and incorporated into the matching.
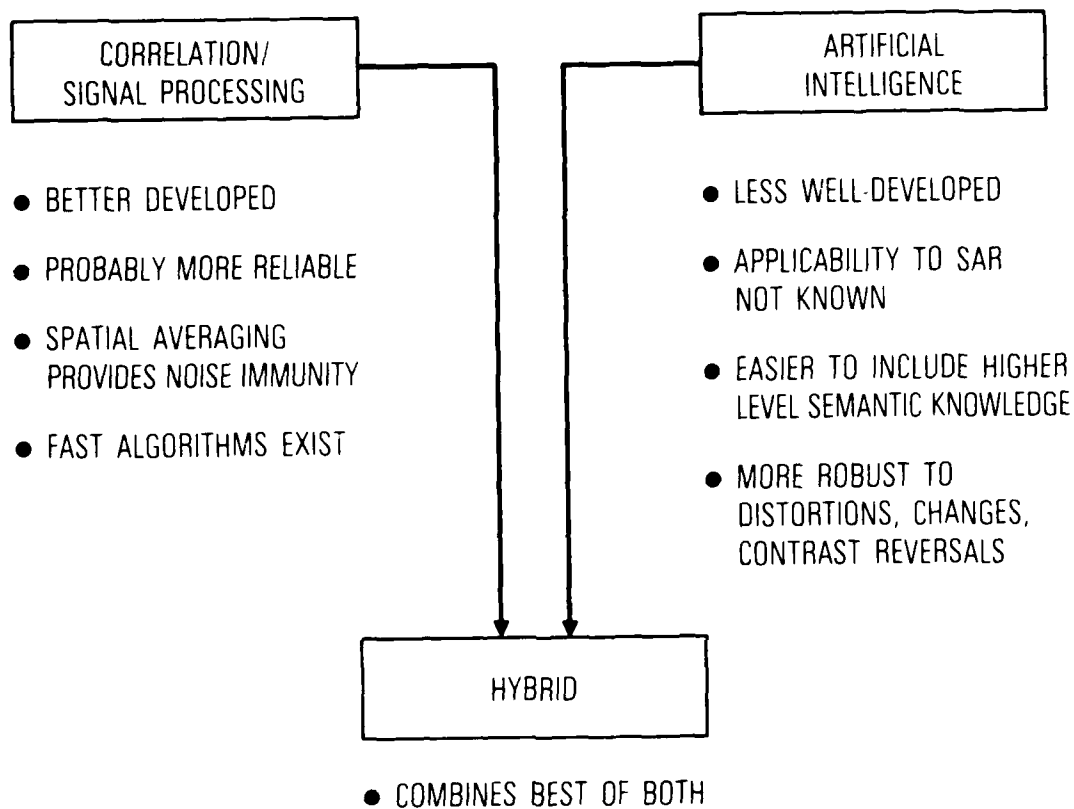
A related problem concerns the matching of SAR images to visible images. In this case, significant contrast reversals between the scenes will occur, thus hybrid or feature matching techniques may be the only ones that work [48].

B.   SAR IMAGE MATCHING ALGORITHMS

Very little work is available on the matching of SAR images to visible reference maps or SAR images. As discussed earlier, most previous work has been concerned with the matching of visible images to visible images. The introduction of speckle scintillation by SAR systems, along with magnification, rotation, geometrical distortion, and other sources of mismatch makes the general SAR matching problem very difficult. This section reviews the few techniques of matching that specifically consider SAR images.

Novak [57,58] has studied a generalized correlation approach to the matching of map reference data to SAR data. He specifically considers the effects of speckle and the reduction of processing complexity using fast implementation techniques. Novak uses correlation with radar edge features (for example, land/water contours, tree/field contours) that have sufficient

66

radar contrast, unique shape, and length to provide reasonable robust perfor-
mance. The actual matching is done with bipolar (+1 or -1) edge or shape
templates such as shown in Figure 22. The unit weights of the template mean
that multiplies are not required, thus reducing the computational complexity.
The template is correlated with the input SAR image, and peaks that exceed a
threshold are recorded along with translational information. For all correla-
tion peaks above a detection threshold, a shape or fill factor equal to the
number of pixels within the +1 template whose value lies above an average of
the template sum is computed. After a search over the whole image, the corre-
lation peak with the largest fill factor is chosen as the best match point.

Several generalizations of the basic correlation method are given by
Novak [57], each having different techniques of computing a correlation
measure. The effect of scintillation and/or speckle is minimized by the
averaging of many resolution cells on each side of the edge template as part
of the correlation. For one particular correlation measure (called "edge
ratio"), Novak derives statistical estimates of the probability of feature
detection and false alarm based on edge contrast ratio, edge length, edge
shape, and template width. He also gives an experimental verification of per-
formance using real SAR data. In another paper [20] Novak extends the pro-
cedure to allow for adaptive detection thresholds (in effect assuming a
spatially nonstationary image model) and considers effects of clutter from
other targets, decoys, or specular reflections.

Hiller [55] has described a shape matching approach for SAR image
matching. Like the techniques described by Novak, Hiller's method has little
dependence on absolute intensity and contrast of the scene. He uses reference
binary templates like that in Figure 22 that are correlated with the input
scenes and exploits the binary characteristics in various ways to achieve
computational savings. The inherent averaging provides resistance to scene
scintillation and speckle. The correlation results are compared to an adap-
tive threshold computed locally over the scene. The adaptive threshold is
effectively self-normalizing and reduces the effects of intensity and contrast
variations. Hiller derives theoretical results on the expected correlation
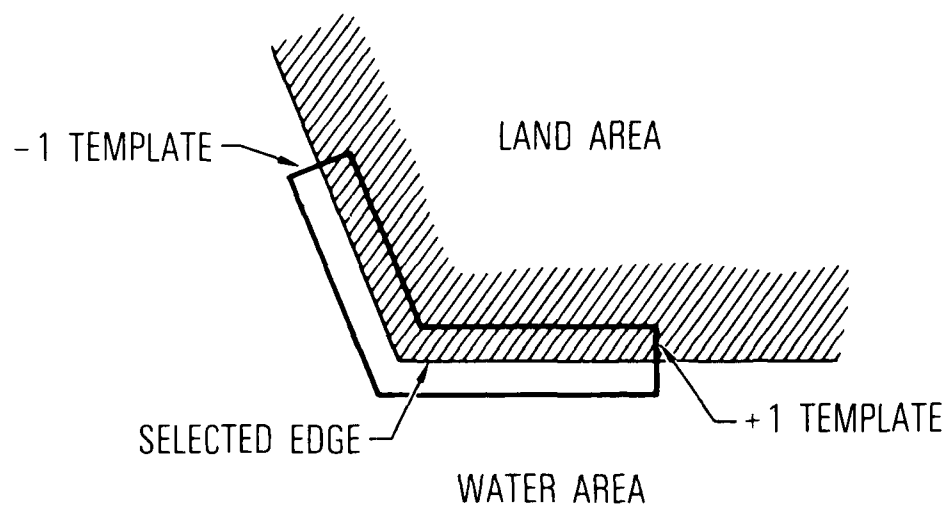value and probability of feature detection as a function of shape parameters.

Figure 22. Bipolar Edge Template for Image Matching

His theory provides a good match with experimental results obtained by correlation over a large ensemble of SAR images.

Kiremidjian has described in several papers [4-6] image-to-map registration algorithms that specifically consider problems of SAR. He is concerned with the registration of 2-D reconnaissance SAR images to a 3-D reference. His presentation is general and is followed later by a discussion of the problems of tactical strip map SAR image matching. Kiremidjian's techniques involve the computation of correspondences between a 2-D SAR image model and a 3-D map data base in terms of a parameter set such as altitude, range, and scale. If the exact values of the parameter set were known, the model then predicts the 2-D SAR image coordinates for any 3-D data base point, and registration is achieved. However, ephemeris data from the sensor platform generally gives estimates of the model parameters. The goals of Kiremidjian's techniques are to refine these estimates so that the location of any data base point can be found in the sensed image within some desired accuracy. Kiremidjian then discusses real-time or near real-time methods for achieving these objectives in a tactical setting.

Two major techniques are given by Kiremidjian. The first [59] requires human operator involvement to pinpoint control point locations in the sensed images. The model predictions of these same control points in the map data base are then compared to the control points obtained by human involvement, and the model parameters are searched for sets of values that minimize the distances between pairs of points.

The second technique [54,59,60] is more automated and relies on the fact that landmarks such as land-water boundaries, roads, and fences produce edges in SAR data. In this procedure, the locations of landmarks in the data base are matched to edges extracted from the SAR image. A search over the model parameters gives the best match.

For both techniques, Kiremidjian gives details of the geometric model for image-to-map registration and describes several algorithms and techniques for parameter refinement and searching. He includes experimental results for both

techniques that prove the differences of the methods. His later papers [54,60] include details of edge extraction, noise suppression and thinning on the SAR image data, and contain a detailed discussion of applications to strip-map SAR imagery with resolution of 512 × 4096 pixels. He demonstrates a location accuracy of 50 m for this type of system. Kiremidjian's work is one of the most complete and relevant references available.

Another study made using assumptions similar to Kiremidjian has been reported by Naraghi and Stromberg [48]. They are also concerned with the matching of SAR imagery to a digital 3-D topographic data base, and matching to previously acquired SAR images. One of their techniques assumes that a known set of matchpoints is extracted by human interaction, and these tie-points alone are used to determine the SAR image distortion. They include a discussion of geometric correction (rubber sheeting) by polynomial matching functions and a mathematical analysis of the geometry connecting 2-D images and 3-D topographic data bases. Another technique given by Naraghi and Stromberg is similar to Kiremidjian's in that platform ephemeris data are combined with tiepoint information for registration. The context of Naraghi and Stromberg's discussion is somewhat different because they concentrate on Seasat SAR data analysis.

VII. PROPOSED NEW TASKS FOR SAR IMAGERY

The first phase of the study objective was to investigate and analyze the general process of rectification. However, in the second phase, the emphasis was placed mostly on the SAR image matching. Part of the objective of the second phase was to propose and develop techniques for registration and change detection with SAR images. These techniques may include SAR image matching to other SAR reference images, to visible references, or to FLIR reference images. Because the problem is generally quite difficult and little work has been previously done on the problem, several approaches are given in the following sections. The results generally apply to both registration (finding of match points for spatial warping) and to change detection once images have been registered. These problems are highly interrelated and differ mainly in the window size over which the matching must be performed.

Based on the analysis in the areas of signal processing and artificial intelligence, four specific tasks are proposed for image registration/rectification and possible change detection of SAR data. The first task involves registration through geometrical transformation and resampling. The second task, which requires considerable research effort, involves total registration and change detection through a combination of signal processing and artificial intelligence techniques. The third task is basically a simplified version of the second task for registration of SAR images with a known, well-defined visible image.

The last task involves man-machine interactive methods for image rectification. System hardware/software requirements and configurations are also discussed for this task. This approach to rectification allows for analytical evaluation and comparison of various registration algorithms and their performance in addition to the utilization of a photointerpreter's inputs to the system.

A. TASK 1 - REGISTRATION THROUGH TRANSFORMATION AND RESAMPLING

The task objective is to develop techniques for registration of SAR imagery in cases where a reference image may not be available (Figure 23). Input may consist of the digital sensed image, some geometric preflight parameters, and calibration data (i.e., geometric control information). Control information may include scanner location and pointing, ground truth, and map transformation.

The method of approach proposed here for digital registration/rectification, consists of two major steps. First, a rectified model is computed from the control information utilizing transformation techniques. Second, the image is warped according to the rectified model through application of resampling and interpolation techniques. For large images, highly specialized computational methods for efficient warping and complicated data processing for error optimization is required. Smaller images or subimages can be handled in a much simpler way. With more preflight and inflight information, higher degree geometrical warping polynomials can be used, and as a result, more accurate registration is expected.

Mathematically, geometrical distortions are mappings from plane to plane that specify where a point in one domain appears in another domain. Section III of this report gives details about the properties of distortion functions and techniques for obtaining them in various applications. Some of the techniques described are: polynomial fit, nearest-neighbor interpolation, finite element method, and the method of potential functions. These are used in cases where there is no need or desire to use a priori knowledge of the nature of the geometric distortion. If one knows (from physical considerations) the general functional form of a distortion, then there are methods (least squares, Kalman filtering, etc.) of fitting the functional form to the observations.

The most complex distortion models arise from sensor geometry correction. Taking the Landsat multispectral scanner (MSS) as a basic example, the raw

72
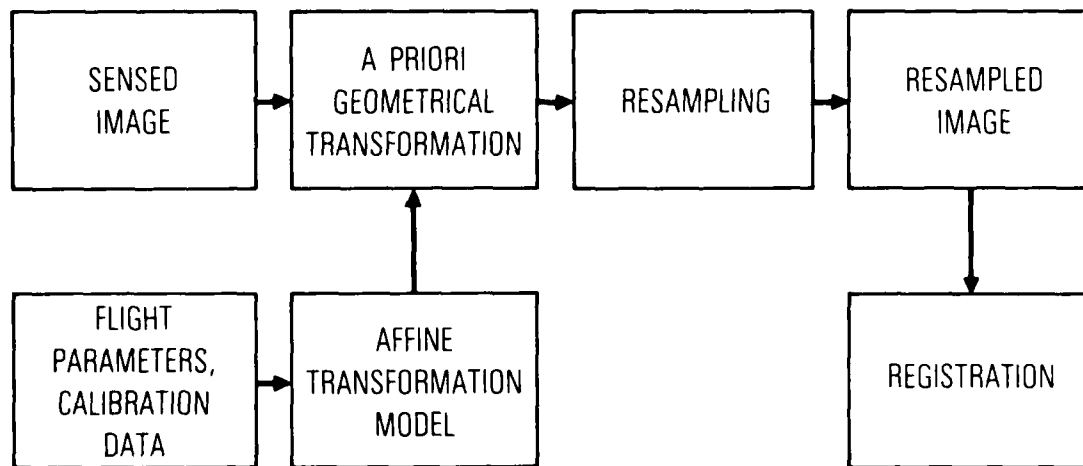
(Reference Map Not Available)

Figure 23. Registration Through Transformation and Resampling

data are perturbed by earth rotation, mirror scan nonlinearity, spherical earth, variations in platform altitude, roll, pitch and yaw. Most of these components can be modeled by continuous functions, but one component, the line-to-line skew induced by earth rotation, is discontinuous at every sixth line. Furthermore, the distortion model is no longer a simple function but a composite of several functions that are applied in order. The first correction function calculates uniform sample spacing in orthographic or Mercator projection along single scan lines. Then a second correction function moves entire lines according to the sensor and earth rotation skew for each line. A third correction for map projection could now be performed if desired.

Two basic techniques for model fitting are in common use today. The first is to use nominal values for spacecraft location, etc., and produce a correlated product which has slight deviations from a perfectly mapped product. Note that the largest deviation is a simple lateral translation, which can be fixed later by a single point observation. The second technique is to fit the model according to control points determined by external means. For our purpose, in which a control point (or reference map) may not be available, the first technique is preferable.

Digital computation requires that the geometric distortion be represented in an efficient manner. The method proposed here is to convert the rectified model to a gridded approximation through the use of resampling methods. There are approximately three techniques commonly used in resampling of one- or two-dimensional data; nearest neighbor, bilinear interpolation, and cubic convolution. These techniques are reviewed in detail in section V.

The above registration/rectification approach requires both analytical and computer simulated modeling. The simplified version (affine transformation plus resampling) can be constructed in four months' time, as a first step toward a more complete modeling.

B. TASK 2 - REGISTRATION AND CHANGE DETECTION OF SAR IMAGES

The task objective is to develop techniques for registration and change detection with SAR images. These techniques may include SAR image matching to

other SAR reference images, to visible references, or to FLIR reference images. Because the problem is generally quite difficult and little work has been previously done on the problem, several approaches are proposed. The results generally apply to both registration and to change detection once images have been registered.

Two major classes of techniques are proposed. The techniques, called A and B, share common techniques in matching and differ mainly in the feature extraction and preprocessing. Because the general matching problem is so difficult and has such a broad application, specialized techniques suitable for a restricted class of situations may be more effective. If specific knowledge about the scope of images to be encountered is available, the general solution may be greatly simplified.

Either of these techniques deserves study and consideration, but both are not well-defined and require considerable research effort. They require significant experimental work, including computer time and the services of a full-time applications programmer in addition to the members of the technical staff who will direct the research.

1.   TECHNIQUE A

This technique of registration is outlined briefly in Figure 24.   SAR images are acquired and smoothed and/or filtered by recursive or nonrecursive image restoration methods [44-48]. Then edge and texture features are extracted. The edges may be linked and expressed as a line segment data base, and the texture features may be obtained by convolution with a set of small window microtexture kernels [49]. These features then go to a segmentation routine that breaks the image into regions of similar characteristics. The shapes of the segmented regions are extracted and form the input to the matching phase of the system. A similar or identical set of operations is performed on the reference image.

The second phase of Technique A is matching. Several major methods are listed; in reality a hybrid approach combining some of them may be used. The method performs shape matching of lines, linear features, vertices, etc., that
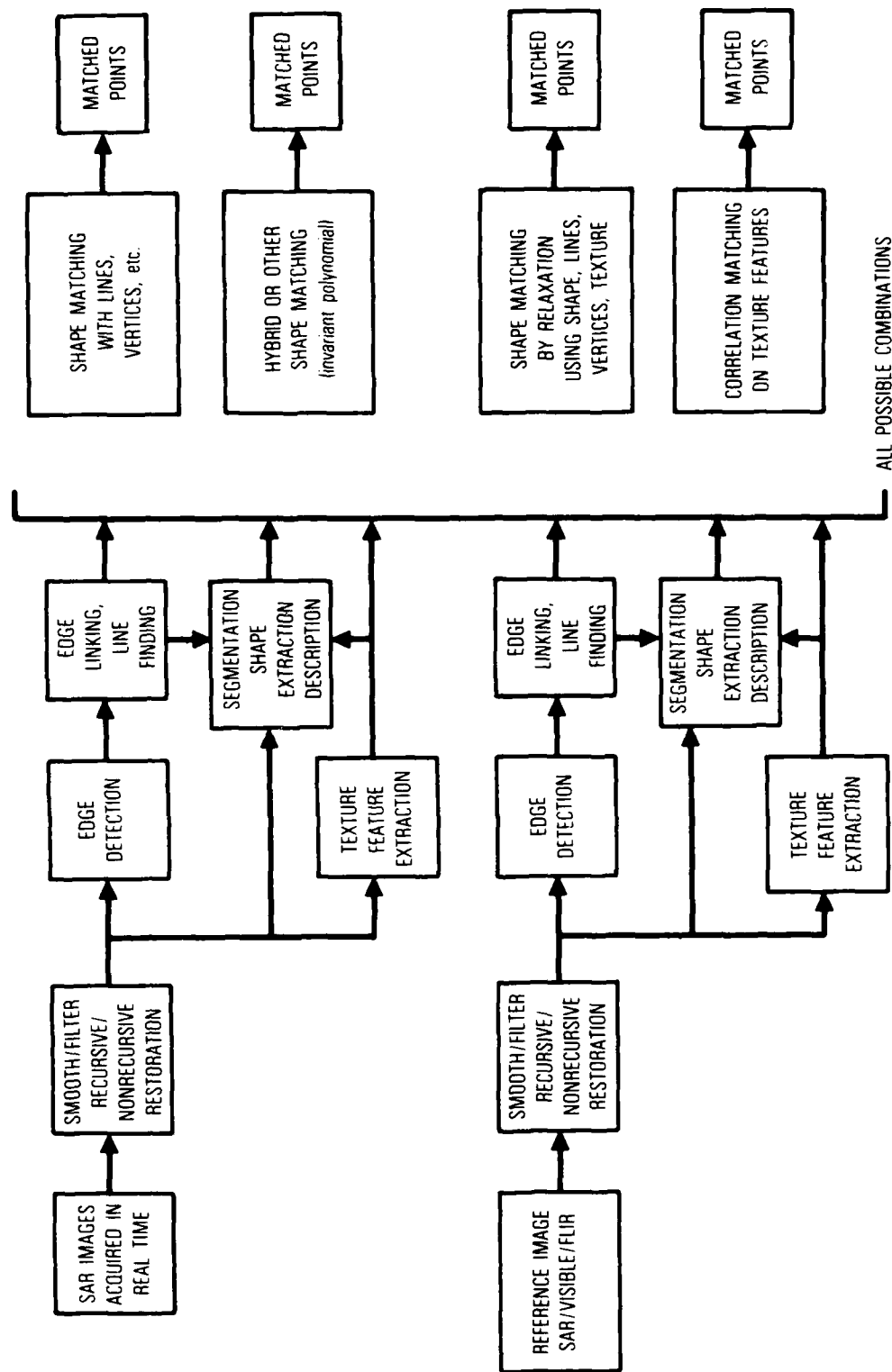
75

Figure 24. Registration Process in Technique A

are stored in a data base. Similar methods have been explored by Hughes
Research Laboratories [17, 51-55] and others. Another method is to match
symbolic descriptions of images, in which the structure is represented by
lines, vertices, higher order shape descriptions, and texture. Techniques
such as relaxation labeling/matching are used to find the best match. For
certain restricted problems, the signal-processing-based techniques of corre-
lation matching may be effective and offer the inherent advantage of noise
reduction. This method may be useful for matching with a well-defined set of
reference images or objects within an image, but will generally fail with
significant changes between reference and image to be matched.

The entire approach of Technique A follows and expands on previously
demonstrated techniques used for visible-to-visible image matching. It is
hoped that the use of noise suppression combined with textural information
will be sufficient for robust performance even though SAR images are signifi-
cantly noisy and different statistically and visually from visible references.

2.   TECHNIQUE B

This technique differs from A in the preprocessing steps. SAR images are
acquired and edge detection/linking is performed as before. Texture feature
extraction is performed, but over a hierarchy of several spatial resolutions
and window sizes (Figure 25). This textural information is input to a segmen-
tation method that attempts to find texture boundaries in the scene. The
texture segmentation is done by unsupervised clustering over the hierarchy of
multiresolution data. This method is motivated by knowledge of the human
visual system, which uses spatial detectors and sensory information over a
range of spatial resolution in order to discriminate texture boundaries. This
area of study is the subject of current research by several groups [57].

Following texture segmentation, shapes are extracted and input to the
various shape matching procedures described before. Reference images
(visible, SAR, FLIR, etc.) are processed by a similar sequence (although less
texture information may be needed for segmenting visible data).

Figure 25. Registration Process in Technique B

78

C. TASK 3 - MATCHING SAR IMAGES TO VISIBLE IMAGES

This task is essentially a simplified version of Task 2 for the registration and matching of SAR images acquired in real-time to a stored visible data base.

The method of approach is basically similar to the two techniques outlined in Task 2, except that we assume the existence of a good quality visible image data-base to which the SAR data are matched. The visible data can consist of stored imagery, extracted features such as lines, edges, segmented regions, and ground control points. Other data, such as previously acquired graphics, roads, physical structures, or map data can be included. Similar features are extracted from the real-time SAR input and are matched as described in Task 2. Following the matching, spatial warping and registration can be performed as described in Task 1.

The advantages of this task as compared with Task 2 is that this is a much simpler problem that can be accomplished with fewer personnel in a shorter amount of time.

D. TASK 4 - MAN-MACHINE INTERACTIVE METHOD

This section discusses proposed man-machine interactive methods for image rectification, system hardware/software requirements, and configurations.

The proposed procedure allows for analytical evaluation and comparison of various registration algorithms and their performance for the specific generic system under consideration. In addition, the new procedure utilizes the inputs of a photointerpreter (PI) and feedback to the system in such a way as to minimize computer storage and computing time requirements.

Most of the rectification methods used in the past ignore the man-machine interaction aspect of the problem or try to make a fully automated rectification process. However, utilization of the PI in the loop may allow for more efficient image registration because the ground truth and specific target areas can be identified in a simpler fashion. The following proposed approach to rectification allows for analytical evaluation and comparison of various

registration algorithms and their performance in addition to the utilization
of a PI's inputs to the system.

1. METHODS OF APPROACH

Onboard sensor data in the form of inflight or preflight information are
available to the various geometrical rectification/registration algorithms.
These data may include limited a priori knowledge of fixed system geometrical
distortions or onboard sensor attitude data. In the new approach proposed
here, general areas of interest for magnification, scale change, comparison
for change detection, etc., are interactively selected from analog hardcopy
images by the PI and used as input to the rectification algorithm. Also,
control point locations corresponding to known areas of the scene and other
points of interest are selected interactively by the PI and used in rectifi-
cation algorithms.

Rectification algorithms proposed here produce geometric corrections
based on existing orientation data and identifiable ground control points
furnished by the PI. Information on the ground control points, furnished by
the PI, could be used in two different fashions: either through parametric
methods or nonparametric methods.

The following is a brief description of the man-machine interactive
methods proposed for the specific system under study. It must be noted that
in practice these methods are applied only to a coarse grid of points distri-
buted through the image. The remaining samples are obtained using resampling
and interpolation procedures for greater efficiency.

a. Orientation Method

In spacecraft-borne sensors, the orientation parameters are continuously
varying functions of time. Thus, to perform good registration of the images,
it is necessary to know these functions with sufficient accuracy. This may he
accomplished in the following manner: approximation, platform stabilization
(costly), interpolation, or geometric modeling. Geometric modeling through
the collinearity condition is proposed here to accomplish sufficient accuracy.

80

The orientation method could use either the preflight data or onboard flight data which are recorded at the same time with the sensed images to generate a new image with all distortions due to aircraft motion removed. These distortions include the roll, pitch, yaw, and translational movements of the platform.

b. Parametric Methods

Parametric methods in rectification make use of a polynomial approximation to relate the original and corrected image coordinates. The ground coordinates of some identifiable points in the image (ground control points) furnished by the PI, combined with least-squares fitting techniques, produce the coefficients of the approximating polynomial.

c. Nonparametric Method

The nonparametric method of rectification is based on the assumption that the difference in coordinates between the original image and the corrected image is a realization of a two-dimensional stochastic field. A simplified version of this approach is proposed here through an arithmetic-mean technique, which for each point computes the difference in coordinates between the original and the corrected image as a weighted average of those differences in a set of ground control points identified by the PI.

2. HARDWARE CONFIGURATION

As noted earlier, the major problem with images presented to the PI is that they differ in magnification, orientation, contrast, etc., due to variations in flight path, sensor response, and ephemeris data. A tactical, ground based image warp correction and registration system with real-time or non real-time speed is needed to implement the correction.

Figure 26 shows a possible system hardware configuration. Figure 26(a) is the part of the system assumed to be conventional SAR processing. Figure 26(b) shows the proposed additional parts of the system that accomplish the necessary rectification/registration of the imagery selected by the PI.

Figure 26(a) shows a block diagram of a typical SAR processing hardware configuration. The sensor system collects data and stores it in analog form
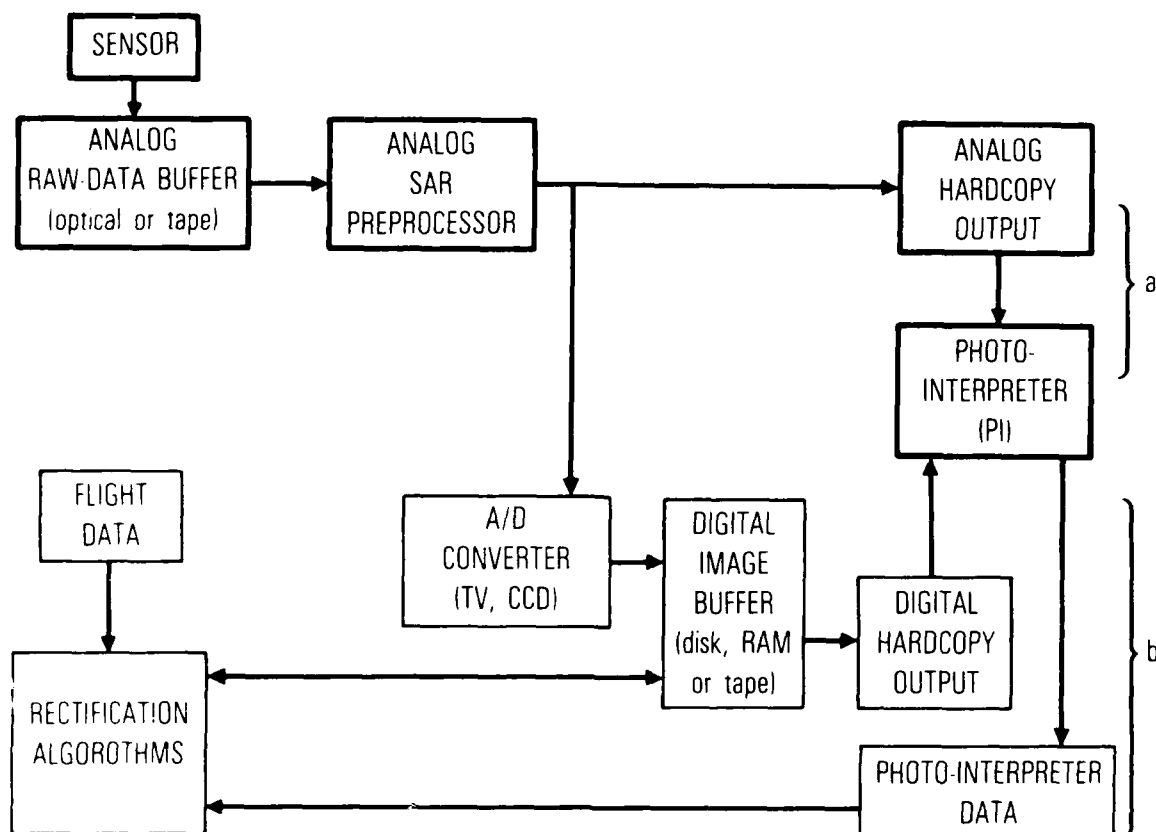
81

Figure 26.   System Hardware Configuration for Man–Machine
Interactive Method (Task 4)

in a raw data buffer. For SAR systems, these data may be stored optically on photographic film or on magnetic tape. An analog SAR processor performs correlation and filtering of the data, giving a hardcopy output with many picture elements (as many as 500 × 500 pixels). A PI views the analog high resolution image and identifies objects of interest and changes as compared with previous images of the same general scene.

Figure 26(b) shows the remaining part of the proposed system utilized for image rectification. Most of the actual correction is implemented digitally. An analog/digital converter (TV, a CCD array, or similar device) is used to digitize analog image outputs and store them in a digital image buffer. The buffer contains sufficient memory to store a few images (on the order of 100) at the resolution needed for comparison with new or existing data by the PI. The buffer may consist of fast access RAM (random access memory) or slower but higher capacity disc or tape digital storage. The buffer also incorporates a computer for implementing the correction and keeping track of the data.

The image buffer/computer uses the selected data provided by the PI (utilizing analog hardcopy images) to establish control points in the digitized digital image data and fit geometrical correction polynomials to control point locations. Interpolation by bilinear or other algorithms is used to compute correction digital images between the control points. The result is a digital hardcopy output of selected areas of the analog scene generally with fewer pixels (on the order of 256 × 256) than the analog scene. The digital output is produced in a form easily overlaid and compared with previously corrected images.

REFERENCES

1. E. H. Conrow and J. A. Ratkovic, "Almost Everything One Needs to Know About Image Matching Systems," Image Proc. for Missile Guidance, SPIE Proc., 238, 426-453 (1980).

2. R. Bernstein, "Digital Image Processing of Earth Observation Sensor Data," Digital Image Proc. for Remote Sensing, IEEE, 55-72 (1978).

3. R. Bernstein and J. Silverman, "Digital Techniques for Earth Resource Image Data Processing," Digital Image Proc. for Remote Sensing, IEEE, 107-120 (1978).

4. J. Markarian, et al., "Implementation of Digital Techniques for Correcting High Resolution Images," Proc. Amer. Soc. Photogrammetry Tech. Sessions and Symp. on Computational Photogrammetry, ASP-ACSM Fall Convention, September 7-11, San Francisco, 285-304 (1971).

5. E. G. Johnston and A. Rosenfeld, "Geometrical Operations on Digitized Pictures," Picture Processing and Psychopictorics, B. S. Kipkin and A. Rosenfeld, eds., Academic Press, New York, 217-240 (1970).

6. J. G. Kawamura, "Automatic Recognition of Changes in Urban Development from Aerial Photography, IEEE Trans. Systems, Man. and Cybernetics, SMC-1, 230-239 (1971).

7. R. L. Lillestrand, "Techniques for Change Detection, IEEE Trans. Computers, C-21, 654-659 (1972).

8. D. G. Luenberger, Optimization by Vector Space Methods, Wiley, New York (1969) pp. 82-83.

9. R. Deutsch, Estimation Theory, Prentice-Hall, Englewood Cliffs, NJ (1965), Ch. 4,5.

10. R. Anuta, "Spatial Registration of Multispectral and Multitemporal Digital Imagery Using Fast Fourier Techniques," IEEE Trans. Geosci. Electron. (October 1970).

11. A. Arcese, P. H. Mengert, and E. W. Trombini, "Image Detection Through Bipolar Correlation," IEEE Trans. Info. Theory, IT-16, 534-541 (1970).

12. W. K. Pratt, "Correlation Techniques of Image Registration," IEEE Trans. Aerosp. Elect. Syst., AES-10, 353-358 (1974).

13. W. K. Pratt, Digital Image Processing, Wiley-Interscience, NY (1978).

14. D. I. Barnea and H. F. Silverman, "A Class of Algorithms for Fast-Image Registration," IEEE Trans. Comp. C-21, 179-186 (1972).

15. B. A. Lambird, D. Lavine, G. C. Stockman, K. C. Hayes, and L. N. Kanal, Study of Digital Matching of Dissimilar Images, ETL-0248, U.S. Army Corps of Engineers, Engineer Topographic Laboratories, Ft. Belvoir (November 1980).

16. B. A. Lambird, D. Lavine, G. C. Stockman, K. C. Hayes, and L. N. Kanal, Analysis and Simulation of Discrete Digital Image Matching, ETL-0278, U.S. Army Corps of Engineers, Engineer Topographic Lab., Ft. Belvoir (November 1981).

17. C. D. Kuglin and W. G. Eppler, "Map-Matching Techniques for Use with Multispectral/Multitemporal Data," Image Proc. for Missile Guidance, SPIE Proc., 238, 146-155 (1980).

18. H. K. Ramapriyan, "A Multilevel Approach to Sequential Detection of Pictorial Features," IEEE Trans. Comp. C-25 (January 1976)

19. R. A. Brooks, and T. O. Binford, "Representing and Reasoning About Partially Specified Scenes," Proc. Image Understanding Workshop, SAI-81-170-WA, Science Applications, Inc., 95-103 (April 1980).

20. D. G. Lowe, and T. O. Binford, "The Interpretation of Geometric Structure from Image Boundaries," Proc. Image Understanding Workshop, Science Applications, Inc., 39-46 (April 1981).

21. R. A. Brooks, R. Greiner, and T. O. Binford, "The ACRONYM Model-Based Vision System," Proc. IJCAI, 105-113 (August 1979).

22. R. Nevatia and K. R. Babu, "Linear Feature Extraction and Description," Proc. IJCAI, 639-641 (August 1979).

23. C. S. Clark, et al., "High Accuracy Model Matching for Scenes Containing Man-Made Structures," Digital Proc. of Aerial Images, SPIE Proc., 186, 54-62 (1979).

24. D. Y. Tseng, et al., "Model-Based Scene Matching," Image Proc. for Missile Guidance, SPIE Proc., 238, 225-231 (1980).

25. S. S. Rifman, et al., Experimental Study of Digital Image Processing Techniques for LANDSAT DATA, Final Report, Report No. 26232-6001-TU-01, TRW Systems, Redondo Beach, CA (January 1976).

26. S. S. Rifman, "Digital Rectification of ERTS Multispectral Imagery," Symposium on Significant Results Obtained from the Earth Resources Technology Satellite-1, Vol. I, Section B (March 1973).

27. R. Bernstein, _All Digital Precision Processing of ERT Images_, Final Report, NASA Contract NAS5-21716 (April 1975).

28. K. W. Simon, "Digital Image Reconstruction and Resampling for Geometric Manipulation," Symposium on Machine Processing of Remotely Sensed Data, LARS, West Lafayette, IN (June 1975).

29. J. H. Ahlberg, E. N. Nilson, and J. L. Walsh, _The Theory of Splines and Their Applications_, Academic Press, 1967.

30. Carl deBoor, _A Practical Guide to Splines_, Springer-Verlag (1978).

31. M. J. Peyrovian, et al., "Image Processing by Smoothing Spline Function," _Proc. Soc. of Photo-Optical Inst. Eng._, 74 (1976).

32. I. E. Abdau and K. Y. Wong, _Fast Nearest-Neighbor 2-Dimensional Interpolation Method_, IBM Technical Disclosure Bulletin (September 1979).

33. H. R. Keshavan and M. D. Srinath, "Two-Dimensional Interpolative Models in Enhancement of Noisy Imager," National Telecommunications Conference, 1977.

34. D. Shepard, "A Two-Dimensional Interpolation Function for Irregularly-Spaced Data," _ACM, Proc. of 23rd Nat. Conf._ (1968).

35. J. Etheridege and C. Nelson, "Some Effects of Nearest Neighbor, Bilinear Interpolation, and Cubic Convolution Resampling on LANDSAT Data," 1979 Machine Processing of Remotely Sensed Data Symposium (1979).

36. L. J. Cutrona, E. N. Leith, L. J. Porcello, and W. E. Vivian, "On the Application of Coherent Optical Processing Techniques to Synthetic Aperture Radar," _Proc. IEEE_, 54, 1026-1032 (August 1966).

37. S. A. Hovanessian, _Introduction to Synthetic Array and Imaging Radars_, Artech House, Dedham, MA (1980).

38. R. O. Harger, _Synthetic Aperture Radar Systems_, Academic Press, New York (1970).

39. K. Tomiyasu, "Review of Synthetic Aperture Radar," _Proc. IEEE_, 563-583 (May 1978).

40. H. Jensen, L. C. Graham, L. J. Porcello, and E. N. Leigh, "Side-Looking Airborne Radar," _Scientific American_, 84-96 (October 1977).

41. Special Issue on Speckle, _J. Opt. Soc. Amer._, 66, (11) (November 1976).

42. J. C. Dainty, ed., _Laser Speckle and Related Phenomena_, Springer-Verlag, Berlin and New York (1975).

43. J. W. Goodman, Introduction to Fourier Optics, McGraw-Hill, New York (1968).

44. D. Kuan, Nonstationary Recursive Restoration of Images with Signal-Dependent Noise with Application to Speckle Reduction, Ph.D. Thesis, Dept. of Elect. Engr., Univ. of So. Calif. (August 1982).

45. D. Kuan, et al., "Nonstationary 2-D Recursive Filter for Speckle Reduction," Proc. IEEE Int. Conf. on Acoustics, Speech and Signal Processing, Paris (May 1982).

46. D. Kuan, et al., "MAP Speckle Reduction Filter for Complex Amplitude Speckle Images," Proc. IEEE Patt. Recog. and Image Proc. Conf., Las Vegas (June 1982).

47. D. Kuan, et al., "Adaptive Restoration of Images with Speckle," Proc. SPIE Tech. Symp. - Appl. of Digital Image Proc. - IV, San Diego (August 1982).

48. N. Naraghi and W. D. Stromberg, "Radar Image Registration and Rectification," Proc. SPIE Tech. Symp. - Appl. of Digital Image Proc. - IV, 359, 86-192 (1982).

49. K. Laws, Textured Image Segmentation, Ph.D. Thesis, Dept. of Elect. Eng., Univ. of So. Cal. (January 1980).

50. C. Elachi, T. Bicknell, R. L. Jordan, and C. Wu, "Spaceborne Synthetic Aperture Imaging Radars: Applications, Techniques and Technology," Proc. IEEE, 70, 1174-1207 (1982).

51. O. D. Faugeras and K. Price, "Symbolic Description of Aerial Images Using Stochastic Labeling," IEEE Trans. Patt. Anal. and Mach. Intell., PAMI-3, 633-642 (1981).

52. C. S. Clark, et al., "High-Accuracy Model Matching for Scenes Containing Man-Made Structures," Proc. SPIE Tech. Symp - Digital Processing of Aerial Images, 186, pp. 54-62.

53. D. Y. Tseng, et al., "Model-Based Scene Matching," Proc. SPIE Tech. Symp. - Image Processing for Missile Guidance, 238, 225-231 (1980).

54. G. K. Kiremidjian, "Registration of a SAR Reconnaissance Image with a Map Reference Data Base," Proc. SPIE Tech. Symp. - Techniques and Applications of Image Understanding, 281, 110-115 (1981).

55. E. R. Hiller, "Pulse-Doppler Map Matching," Proc. SPIE Tech. Symp. - Image Processing for Missile Guidance, 238, 50-58 (1980).

56. E. H. Adelson and P. Burt, "Image Data Compression with the Laplacian Pyramid," Proc. IEEE Comp. Soc. Conf. on Patt. Recognition and Image Proc., Dallas, 218-223 (August 1981).

57. L. M. Novak, "Correlation Algorithms for Radar Map Matching," IEEE Trans. Aerosp. and Elect. Syst., AES-14, 641-648 (1978).

58. L. M. Novak, "Radar Target Detection and Map-Matching Algorithm Studies," IEEE Trans. Aerosp. and Elect. Syst., AES-16, 620-625 (1980).

59. G. Kiremidjian, "Image-to-Map Registration," Image Proc. for Missile Guidance, Proc. SPIE, 238, 184-193 (1980).

60. G. Kiremidjian, "Radar Image-to-Map Registration," Optical Engineering, 20, 899-906 (1981).

END

FILMED

10-85

DTIC